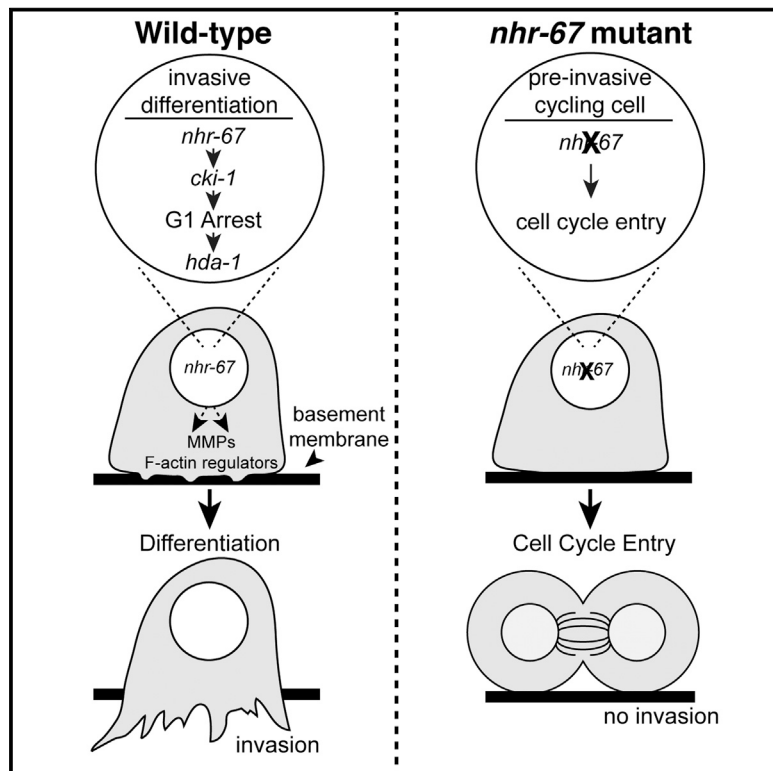


Developmental Cell

Invasive Cell Fate Requires G1 Cell-Cycle Arrest and Histone Deacetylase-Mediated Changes in Gene Expression

Graphical Abstract



Authors

David Q. Matus, Lauren L. Lohmer, Laura C. Kelley, ..., Wan Zhang, Qiuyi Chi, David R. Sherwood

Correspondence

david.matus@stonybrook.edu (D.Q.M.), david.sherwood@duke.edu (D.R.S.)

In Brief

Functional links between cell-cycle arrest and invasive behavior have been difficult to show in vivo. Here, Matus et al. use *C. elegans* to demonstrate that cell invasion is a differentiated cellular state that requires G1 arrest, regulated by the transcription factor NHR-67/TLX and HDAC-mediated changes in gene expression.

Highlights

- NHR-67/TLX maintains the *C. elegans* invasive anchor cell (AC) in G1 arrest
- Mitotic ACs downregulate CKI-1/p21CIP1 and fail to invade
- Mitotic ACs express early markers but lack differentiated invasive genes
- Downstream of G1 arrest, invasive differentiation requires the HDAC, HDA-1



Invasive Cell Fate Requires G1 Cell-Cycle Arrest and Histone Deacetylase-Mediated Changes in Gene Expression

David Q. Matus,^{1,3,*} Lauren L. Lohmer,¹ Laura C. Kelley,¹ Adam J. Schindler,¹ Abraham Q. Kohrman,³ Michalis Barkoulas,² Wan Zhang,³ Qiuyi Chi,¹ and David R. Sherwood^{1,*}

¹Department of Biology, Duke University, Box 90338, Durham, NC 27708, USA

²Department of Life Sciences, Imperial College London, Imperial College Road SAF Building, London SW7 2AZ, UK

³Department of Biochemistry and Cell Biology, Stony Brook University, Stony Brook, NY 11794-5215, USA

*Correspondence: david.matus@stonybrook.edu (D.Q.M.), david.sherwood@duke.edu (D.R.S.)

<http://dx.doi.org/10.1016/j.devcel.2015.10.002>

SUMMARY

Despite critical roles in development and cancer, the mechanisms that specify invasive cellular behavior are poorly understood. Through a screen of transcription factors in *Caenorhabditis elegans*, we identified G1 cell-cycle arrest as a precisely regulated requirement of the anchor cell (AC) invasion program. We show that the nuclear receptor *nhr-67/tlx* directs the AC into G1 arrest in part through regulation of the cyclin-dependent kinase inhibitor *cki-1*. Loss of *nhr-67* resulted in non-invasive, mitotic ACs that failed to express matrix metalloproteinases or actin regulators and lack invadopodia, F-actin-rich membrane protrusions that facilitate invasion. We further show that G1 arrest is necessary for the histone deacetylase HDA-1, a key regulator of differentiation, to promote pro-invasive gene expression and invadopodia formation. Together, these results suggest that invasive cell fate requires G1 arrest and that strategies targeting both G1-arrested and actively cycling cells may be needed to halt metastatic cancer.

INTRODUCTION

During morphogenetic processes in development and in diseases such as cancer, cells acquire the specialized ability to invade into other tissues. One of the most significant barriers invasive cells encounter is basement membrane (BM), a thin, dense, highly crosslinked extracellular matrix that surrounds most tissues (Rowe and Weiss, 2008). The acquisition of invasive behavior is accompanied by changes in gene expression, such as upregulation of matrix metalloproteinases (MMPs), actin regulators, and the expression of genes that promote the formation of invadopodia, dynamic membrane-associated F-actin structures that breach BM (Eckert et al., 2011; Kelley et al., 2014; Page-McCaw et al., 2007; Wang et al., 2004). Transcriptional programs are thought to be crucial in driving the expression of genes that endow invasive cells with their specialized character-

istics (Ozanne et al., 2006). Due to the challenge of studying invasion in complex tissue environments in vivo, the identity and function of these transcriptional regulators remains poorly understood.

C. elegans anchor cell (AC) invasion is a visually and genetically accessible model for revealing mechanisms controlling invasion (Matus et al., 2010; Sherwood et al., 2005; Sherwood and Sternberg, 2003). During the third larval stage (L3) of larval development, the AC, a specialized uterine cell, breaches the BM separating the uterine and vulval tissues and contacts the vulval cells to initiate uterine-vulval connection. AC invasion is coordinated with the underlying vulval precursor cell P6.p divisions: the AC is specified at the P6.p one-cell stage, initiates invasion at the P6.p two-cell stage, and completes invasion at the P6.p four-cell stage (Sherwood and Sternberg, 2003). Prior to invasion, a number of genes are upregulated in the AC that contribute to BM breaching, including the MMP *zmp-1*, actin regulators, and the extracellular matrix component hemicentin (Morrissey et al., 2014; Sherwood et al., 2005; Wang et al., 2014; Ziel et al., 2009). Further, similar to metastatic cancer cells, the AC forms invadopodia that breach the BM (Hagedorn et al., 2013, 2014).

Prior to and during AC invasion, the neighboring uterine cells proliferate. The AC, however, never divides, suggesting that its cell cycle is uniquely regulated (Figure 1A). This feature appears to be highly conserved, as previous studies examining nematode species that last shared a common ancestor ~280–430 million years ago showed that all have a single non-dividing invasive AC (Félix and Sternberg, 1996; Matus et al., 2014). Notably, although metastatic cancer is associated with proliferation and invasion through BM (Valastyan and Weinberg, 2011), invasive ability is correlated with the attenuation of cell proliferation in a number of cancer cell lines, tumor models, and at the invasive front of human colorectal and basal cell carcinomas (Gil-Henn et al., 2013; Hoek et al., 2008; Patsos et al., 2010; Rubio, 2008; Svensson et al., 2003; Wang et al., 2004; Yano et al., 2014). Neural crest cells undergoing epithelial-mesenchymal transition (EMT), a process that involves BM breaching, also show reduced proliferation during EMT, followed by a proliferative phase after EMT is complete (Kelley et al., 2014; Ridenour et al., 2014; Vega et al., 2004). These observations suggest a possible connection between cell proliferation and invasion; however, a functional link between invasive ability and loss of proliferation

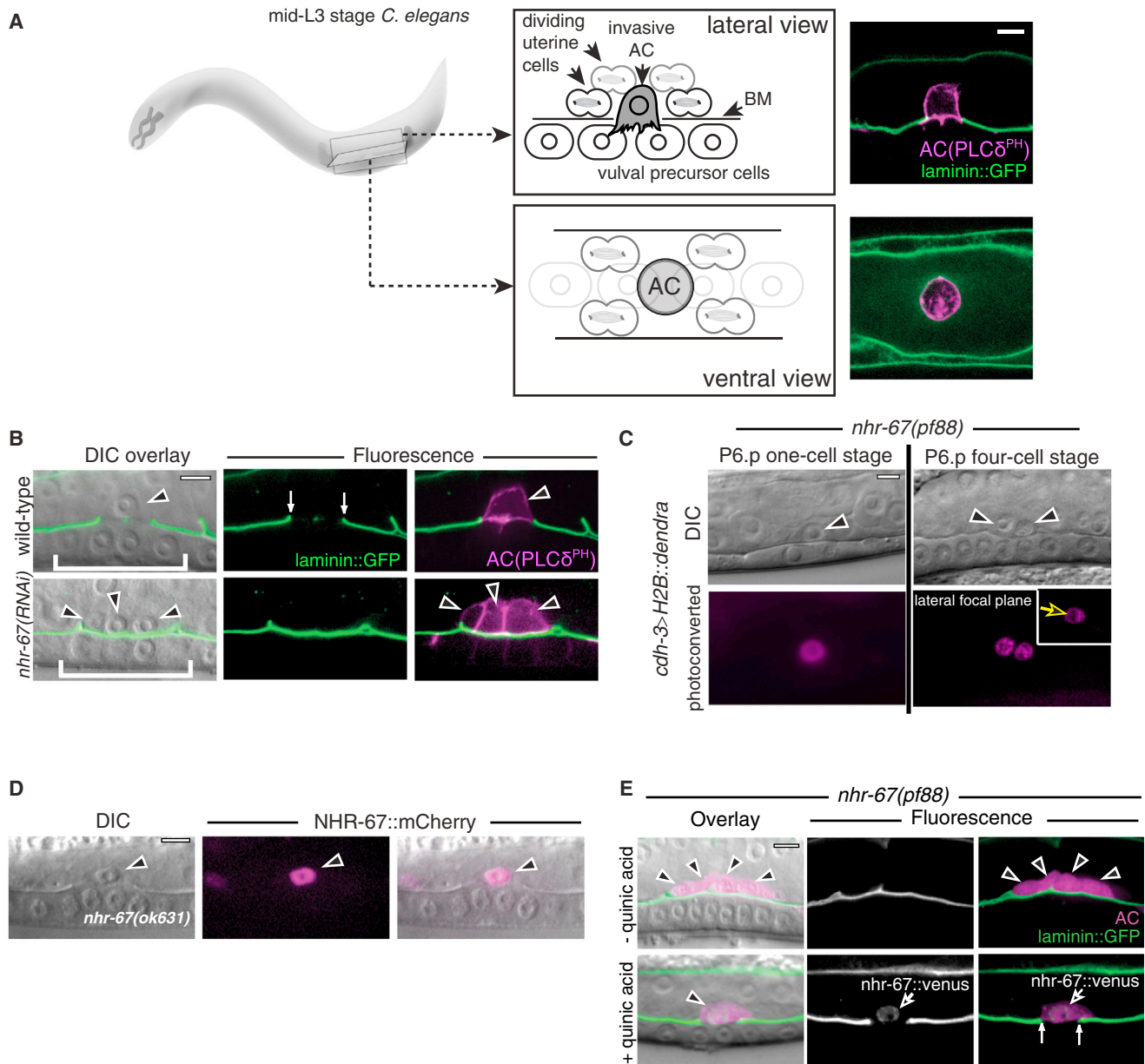


Figure 1. *nhr-67* Promotes AC Invasion and Prevents AC Proliferation

(A) Schematic diagram and micrographs depicting the two perspectives used for imaging AC invasion. During the mid-to-late L3 stage (left), the uterine AC (magenta) breaches the BM (green) to contact the vulval precursor cells (diagram, middle). The single plane of confocal z stack (right) depicts lateral (top) and ventral (bottom) views of the AC invasion.

(B) BM marker (laminin::GFP) overlaid on DIC (left) and corresponding fluorescence (middle). The AC-specific membrane (*cdh-3^{1.5}>mCherry::PLC δ^{PH}* , magenta) and BM marker (right) are shown. The AC(s) (arrowheads) and BM breach (arrows) in the wild-type (top) and multiple non-invading ACs following *nhr-67(RNAi)* depletion (bottom) are shown.

(C) A single H2B::Dendra-expressing AC was photoconverted (left, top DIC and bottom fluorescence) at the P6.p one-cell stage and gave rise to three ACs by the P6.p four-cell stage (right).

(D) DIC image (left), fluorescence (middle), and overlay (right) show NHR-67::mCherry in the AC nucleus of an *nhr-67* mutant animal expressing *nhr-67>NHR-67::mCherry*.

(E) Early AC-specific nuclear localization of NHR-67::venus (arrowhead, bottom middle and bottom right) using the Q system (Wei et al., 2012) rescued AC invasion and prevented proliferation in all *nhr-67(pf88)* mutants (top) (see also Table S3). The scale bars represent 5 μ m. See also Figure S1 and Movie S1.

has not been established. Further, the possible mechanistic reasons that might require invasive cells to arrest or exit the cell cycle are unknown. This is particularly important to understand

in regards to metastatic cancers that, similar to neural crest cells, reversibly switch between proliferative and non-dividing states (Hoek et al., 2008). Given that current chemotherapies primarily

target actively dividing tumor cells (Yano et al., 2014), these treatments would potentially leave non-dividing invasive cells unaffected and capable of repopulating tumors after re-entering the cell cycle at a later time.

Cell differentiation requires changes in gene transcription that depend upon chromatin remodeling (De Falco et al., 2006; de la Serna et al., 2006; Yuzyuk et al., 2009). These alterations in transcription are thought to be incompatible with the switching off of gene expression that occurs during active cell division (Ma et al., 2015; Singh et al., 2013). This is likely one reason that the G1 cell-cycle phase, an interphase growth state that is often prolonged or arrested, is coupled to the differentiation of many cell types during development (Buttitta et al., 2007). Although invasive cells have distinct gene expression profiles (Berthier-Vergnes et al., 2011; Wang et al., 2004), it is currently unclear if these cells adopt an invasive differentiated cell fate that requires G1 cell-cycle arrest.

Through an RNAi screen of *C. elegans* transcription factors, we identify here the conserved nuclear hormone receptor NHR-67/TLX as a critical regulator of AC invasion. Loss of *nhr-67* resulted in dividing non-invading ACs that express early markers of AC specification. Examination of cell-cycle markers revealed that NHR-67 maintains the AC in G1 arrest, in part through regulation of the cyclin-dependent kinase inhibitor *cki-1*. We show that *nhr-67*-deficient ACs that enter the cell cycle lack invadopodia and fail to express MMPs and actin regulators that promote invasion. We further find that the histone deacetylase (HDAC), *hda-1*, a key regulator of chromatin remodeling and cellular differentiation, is upregulated in the AC after G1 arrest and promotes pro-invasive gene expression and invadopodia formation. These results suggest that the invasive cell fate of the AC is a differentiated cellular state requiring G1 arrest and HDAC mediated changes in gene expression.

RESULTS

A Transcription Factor RNAi Screen Identifies *nhr-67/tlx* as a Regulator of AC Invasion

To identify transcriptional programs that regulate AC invasion, we screened an RNAi library of 854 transcription factors (86% of *C. elegans* transcription factors) in a strain where only the uterine cells are sensitive to RNAi (Table S1). This tissue specific RNAi sensitivity was achieved with uterine-specific rescue of the Argonaute/PIWI gene *rde-1* in an *rde-1* mutant background (Haerty et al., 2008; Hagedorn et al., 2009). We identified genes whose reduction resulted in a protruding vulval (Pvl) phenotype (Table S2), which can indicate an AC invasion defect (Matus et al., 2010) and is easily observed under a stereomicroscope as a protuberance on the ventral surface of adult hermaphrodites. Loss of the conserved orphan nuclear hormone receptor *nhr-67/tlx* (Verghese et al., 2011), which has not been previously implicated in AC invasion, resulted in the highest observance of PvlS (Table S2). Examination of AC invasion after *nhr-67* depletion in the uterine-specific RNAi strain containing the BM marker laminin::GFP with the early AC specification reporter *cdh-3* revealed the presence of approximately 75% of animals with multiple non-invading ACs and 25% of animals with single ACs that invaded normally (Figure 1B; Table S3) (Sherwood and Stern-

berg, 2003). An *nhr-67* null allele has not been isolated and deletion alleles of *nhr-67* (*ok631* and *tm2217*) were either embryonic or early larval lethal (*ok631*) or not viable for scoring at the time of AC invasion (*tm2217*) (Verghese et al., 2011). Thus, in order to confirm our RNAi result, we examined animals harboring a hypomorphic allele of *nhr-67* (*pf88*), which contains a 389-bp deletion in the *nhr-67* promoter (Verghese et al., 2011). This *nhr-67* mutant had a similar percentage of multiple non-invasive *cdh-3* expressing cells as well as single invasive ACs as *nhr-67* RNAi depleted animals (Table S3) (Verghese et al., 2011). Targeted reduction of *nhr-67* by RNAi in *nhr-67*(*pf88*) animals did not significantly change the number of animals possessing multiple non-invading ACs (Table S3), suggesting that the *nhr-67*(*pf88*) allele is a strong loss-of-function or functional null allele for the AC phenotype.

Loss of NHR-67 Results in Proliferating ACs

We hypothesized that the presence of multiple cells expressing the AC reporter after loss of *nhr-67* could arise either from neighboring uterine cells acquiring the AC fate or from proliferation of the normally non-dividing AC. To determine the origins of the additional cells, we established transgenic worms expressing an AC specific photoconvertible histone::dendra tag (using the promoter for *cdh-3*, *cdh-3*>H2B::dendra) as a means to lineage trace ACs over developmental time (Gurskaya et al., 2006). Shortly after the time of AC specification (approximately 5 hr before invasion), we found that there was a single AC expressing histone::dendra in most *nhr-67*(*pf88*) mutants (Figures 1C and S1A). Laser directed killing of the AC at this time resulted in the absence of ACs during the period of invasion (Figure S1B). These results suggest that the AC is specified normally, but then it and its descendants divide after loss of *nhr-67*. Consistent with this notion, optical highlighting revealed that the single ACs present at the time of specification usually divided and gave rise to between three and nine ACs in *nhr-67* mutants (Figures 1C and S1A). Time-lapse microscopy confirmed that ACs divided after loss of *nhr-67* (Movie S1). Taken together, these results indicate that *nhr-67* prevents division of the AC after its specification.

NHR-67 Functions in the AC to Prevent AC Division and Promote Invasion

To explore how NHR-67 functions to regulate AC division and invasion, we first examined a recombiner functional *nhr-67* reporter (*nhr-67*>NHR-67::mCherry) (Sarin et al., 2009; Verghese et al., 2011). *nhr-67*>NHR-67::mCherry was initially detected in the nucleus of four ventral uterine (VU) cells in the early L2 somatic gonad (Figure S1C), including the future AC (Kimble and Hirsh, 1979). Following AC specification, *nhr-67*>NHR-67::mCherry became enriched in the AC nucleus and was lost in neighboring uterine cells (Figure 1D), suggesting that NHR-67 might function directly in the AC. To test this notion, we utilized the Q-system (Wei et al., 2012) to induce AC-specific expression of NHR-67::venus shortly after AC specification (see Supplemental Information). AC-specific expression of NHR-67 prevented AC divisions and fully restored invasion in *nhr-67*(*pf88*) mutants (Figure 1E; Table S3). Thus, NHR-67 functions within the AC after its specification to prevent AC division and to promote invasion.

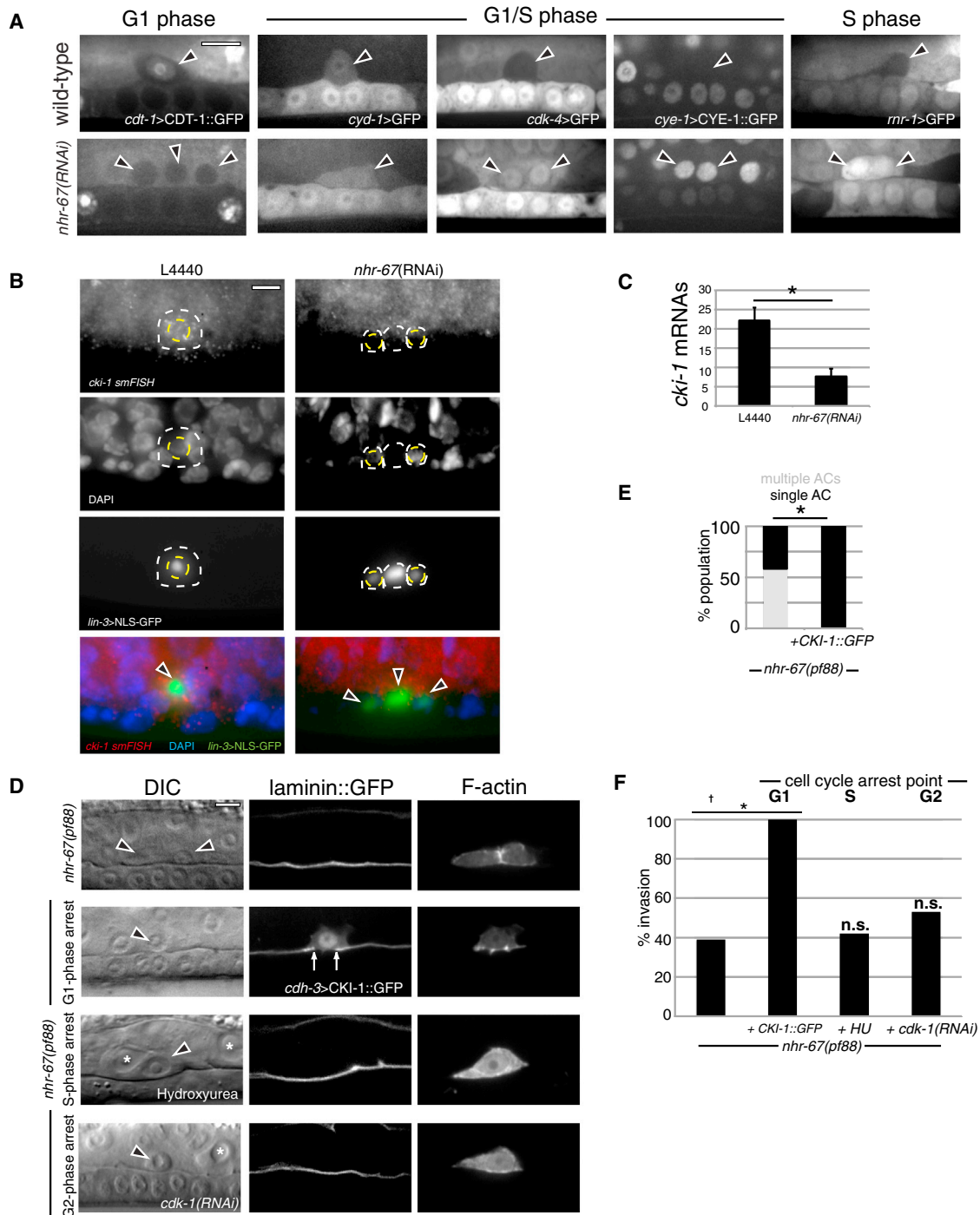


Figure 2. CKI-1-Induced G1 Arrest Rescues Invasion in *nhr-67*-Deficient ACs

(A) Confocal sections of cell-cycle GFP reporters in wild-type (top) and *nhr-67(RNAi)*-treated animals (bottom).

(B) Epifluorescence smFISH images depict localization of *cki-1* transcripts (grayscale, top and red in overlay, bottom), nuclei (grayscale, second row and blue in overlay, bottom), and an AC-specific reporter (*lin-3>NLS-GFP*, grayscale, third row and green in overlay, bottom). The AC in the *nhr-67(RNAi)*-depleted animals is undergoing mitosis and thus lacks DAPI staining and an intact nucleus. Thus, the NLS-GFP is present throughout the cell. The white lines indicate the position of the AC and the dashed yellow lines indicate the position of the AC nuclei.

(C) Quantification of *cki-1* mRNA transcripts per AC by smFISH ($n > 10$ animals examined for each, $*p < 0.002$, by a Student's *t* test, and error bars represent SEM).

(D) DIC micrographs (left) and corresponding confocal sections of BM (laminin::GFP, middle) and an AC-specific F-actin probe (*cdh-3>mCherry::moesinABD*, right) at the normal time of AC invasion. An *nhr-67(pf88)* animal has two ACs (arrowheads) that fail to invade (top). Induction of G1-phase arrest (*cdh-3>CKI-1::GFP*, second row) blocked cell division and rescued BM invasion (arrows). Induction of S phase arrest (hydroxyurea, third row) or G2-phase arrest (*cdk-1(RNAi)*, bottom) blocked AC division and division of uterine cells (*), but did not rescue invasion (intact laminin::GFP, middle).

(legend continued on next page)

NHR-67 Promotes G1 Arrest through Regulation of *cki-1*

To determine how NHR-67 regulates the cell cycle in the AC, we analyzed markers of cell-cycle progression. All wild-type ACs showed nuclear localization of *cdt-1*>CDT-1::GFP (Figure 2A), a marker for cells in the G1 phase (Kim and Kipreos, 2007; Matus et al., 2014). Wild-type ACs also expressed the sole cyclin D ortholog *cyd-1* (Figure 2A), which is also predominantly expressed in G1 (Park and Krause, 1999). We failed to detect the G1/S phase reporters *cdk-4*>GFP and *cye-1*>CYE-1::GFP (cyclin E) and the S phase reporter *rnr-1*>GFP, whose expression is indicative of actively cycling cells ($n > 10/10$ animals for each marker; Figure 2A) (Fujita et al., 2007; Park and Krause, 1999). Finally, using single molecule fluorescent in situ hybridization (smFISH), high levels of transcript for *cki-1* (Cip/Kip family CDK inhibitor), which promotes G1 arrest, were found in the AC (Figures 2B and 2C) (Hong et al., 1998). The lack of AC divisions and expression of markers of G1 and G1 arrest suggest that in wild-type animals the AC is arrested in G1.

To determine if *nhr-67* maintains the AC in G1 arrest, we examined cell-cycle markers after RNAi depletion of *nhr-67*. While single-invading ACs always expressed nuclear *cdt-1*>CDT-1::GFP, a marker for G1 arrest ($n = 10/10$ animals), the multiple non-invading ACs present after *nhr-67* reduction lost nuclear *cdt-1*>CDT-1::GFP and expressed the G1/S and S phase markers *cdk-4*>GFP, *cye-1*>CYE-1::GFP, and *rnr-1*>GFP ($n > 10/10$ animals for each; Figure 2A). We conclude that NHR-67 promotes G1 arrest in the AC.

Cyclin-dependent kinase inhibitors are often upregulated in cells to help trigger G1 cell-cycle exit (Buttitta and Edgar, 2007). To examine whether NHR-67 may directly regulate *cki-1* expression in the AC to promote G1 arrest, we first examined the *cki-1* upstream regulatory region. NHR-67 is an NR2E1-class transcription factor that binds DNA at a single conserved AAGTCA hexamer site (Sarin et al., 2009). Notably, there are six AAGTCA sites in a 5.3 kb region of genomic DNA ~9 kb away from the transcriptional start site of *cki-1* (Figure S2A), raising the possibility that *cki-1* is a direct target of NHR-67. This genomic region, however, failed to drive GFP expression in the AC when fused to a GFP minimal reporter. We also did not detect AC expression in a full-length translation reporter, *cki-1*>CKI-1::GFP (Figure S2A and data not shown), suggesting that the AC regulatory element is complex. We therefore examined endogenous transcripts of *cki-1* in the AC (Figure 2B). In support of NHR-67 transcriptional regulation of *cki-1*, we detected a 2.9-fold decrease in endogenous transcript levels of *cki-1* following *nhr-67*-depletion (Figures 2B and 2C). We also found that RNAi depletion of *cki-1* in a uterine-specific RNAi strain resulted in dividing ACs, but only in rare cases compared to loss of *nhr-67* ($n = 3$ occurrences out of > 100 animals observed; Figure S2B). Taken together, these results suggest that NHR-67 promotes G1 arrest in the AC through regulation of *cki-1* and likely another unknown effector(s).

Induced G1 Arrest Rescues *nhr-67*-Deficient AC Invasion

Our results indicated that NHR-67 promotes G1 arrest and AC invasion. To determine if these functions are directly linked, we triggered G1 arrest in the AC in *nhr-67* mutant animals by driving AC-specific expression of CKI-1::GFP (Hong et al., 1998; Matus et al., 2014). Strikingly, CKI-1 expression completely rescued AC invasion in *nhr-67*(*pf88*) hypomorphs (Figures 2D and 2E; Table S3). Importantly, a form of CKI-1 lacking conserved residues required to bind and inhibit cyclin/CDK complexes (Vlach et al., 1997) failed to block division or rescue invasion, demonstrating that G1 arrest, and not another function for CKI-1, is required to promote invasion (Figures S2C–S2E; Table S3). We further found that arrest of the AC in the S phase via either hydroxyurea treatment or depletion of the sole PCNA ortholog, *pcn-1*, or arrest in G2 phase through depletion of *cdk-1* by RNAi in *nhr-67* mutants failed to rescue invasion (Figures 2D, 2F, and S2F; Table S3) (Nusser-Stein et al., 2012; Sonnevile et al., 2015). Taken together, these results indicate that NHR-67 promotes AC invasion by specifically directing the AC into G1 arrest.

G1 Arrest Is Required for Invadopodia Formation and Pro-invasive Gene Expression

To understand the link between G1 arrest and invasion, we examined the specialized invasive characteristics of the AC after loss of *nhr-67* in the dividing ACs. While wild-type ACs formed numerous invadopodia, *nhr-67*-depleted ACs failed to generate invadopodia, regardless of cell-cycle state, as there was no significant difference in number of invadopodia between actively dividing and interphase ACs (Figures 3A–3C) (Hagedorn et al., 2013). Furthermore, loss of *nhr-67* resulted in the absence or reduction of expression of the pro-invasive MMP *zmp-1* and the conserved matrix gene *him-4* (Figure 4A) (Matus et al., 2010; Sherwood et al., 2005). We also found that two additional MMPs expressed in the AC, *zmp-3* and *zmp-6*, were dependent on *nhr-67* (Figures 4A and 4B). Finally, we examined the expression of actin regulators that promote invasive cellular behavior (Li et al., 2014; Wang et al., 2014). We found that AC expression of the actin regulators *exc-6* (formin) and *unc-34* (Ena/VASP) was dependent on NHR-67 activity, as RNAi depletion of *nhr-67* resulted in reduced expression of *exc-6* and *unc-34* GFP transcriptional reporters (Figures 4A and 4B). Consistent with these specialized invasive traits of the AC being reliant on G1 arrest, AC-specific expression of *cki-1* in *nhr-67*(*pf88*) animals restored invadopodia (Figures 3B and 3D) and MMP expression (Figures 4C and 4D). Importantly, early markers of AC specification were detected in the dividing ACs after loss of *nhr-67*, including the fat-like cadherin *cdh-3*, the integrin *pat-3*, and the EGF-like ligand *lin-3* (Figures 4A, 4B, and S3) (Sherwood et al., 2005). During development, G1 arrest is associated with the differentiation of specialized cell fates (Sarkar et al.,

(E) Bar graph depicts the percentage of the population of *nhr-67*(*pf88*) and *nhr-67*(*pf88*); *cdh-3*>CKI-1::GFP animals with single versus multiple ACs ($n > 50$ animals examined for each condition and $*p < 1 \times 10^{-12}$, by a two-tailed Fisher's exact test).

(F) Percentage of invading ACs in *nhr-67*(*pf88*) animals and following cell-cycle phase-specific arrest ($n > 50$ animals each; † all *nhr-67*(*pf88*) non-invading ACs are mitotic and invading ACs are G1 arrested; see also Table S3; Figure S2; $*p < 0.0001$; not significant, n.s.; $p = 1$, HU treatment; $p = 0.59$; *cdk-1*(RNAi) as compared to *nhr-67*(*pf88*) alone; and by a two-tailed Fisher's exact test). The scale bars represent 5 μ m. See also Figure S2.

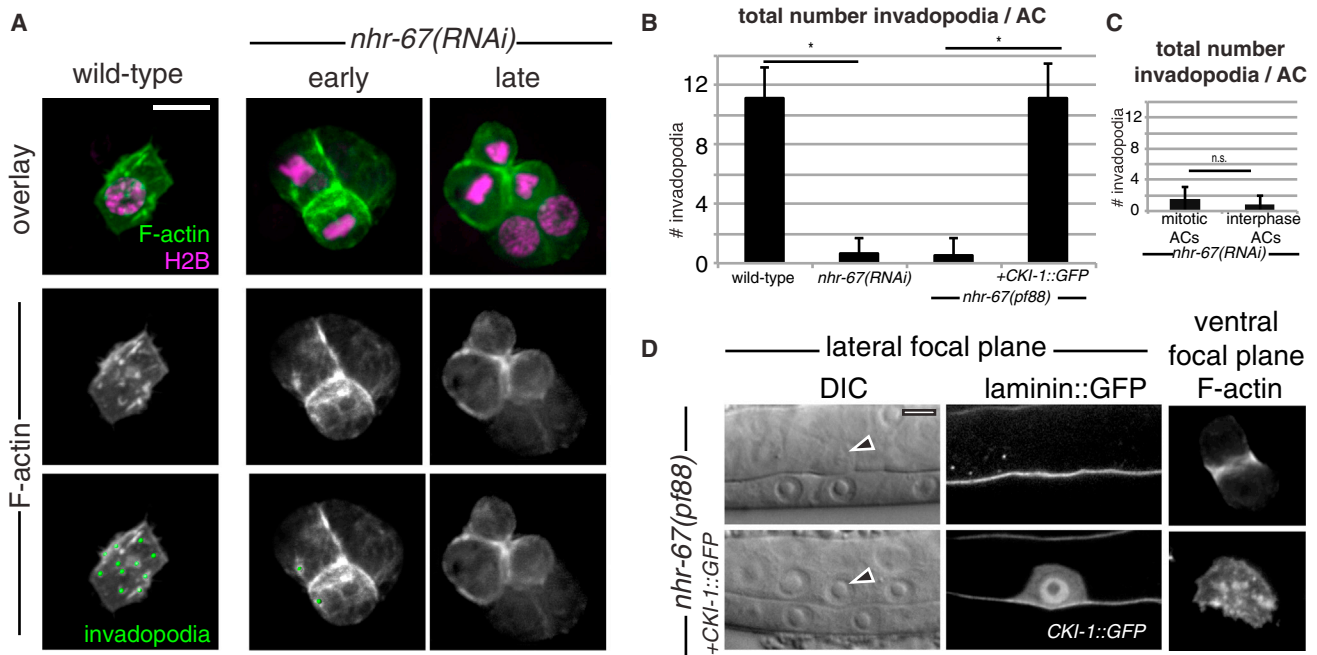


Figure 3. G1 Arrest Is Required for Invadopodia Formation

(A) Ventral projection of confocal z stacks showing punctate F-actin-rich invadopodia along the basal surface of the AC in wild-type (left) and in dividing ACs of a *nhr-67(RNAi)*-treated (right) animal. *nhr-67(RNAi)*-depleted animals were imaged prior to the normal time of invasion (middle) and approximately 1 hr later (late). The fluorescence overlay (top) shows F-actin (*cdh-3>mCherry::moesinABD*, green) and histone (*cdh-3>H2B::GFP*, magenta) and F-actin alone (grayscale, middle and bottom) with green spots (bottom) assigned to invadopodia.

(B) Quantification of invadopodia number in wild-type ($n = 13$ ACs examined and 11 ± 2 structures present) as compared to *nhr-67(RNAi)*-treated animals ($n = 31$ dividing ACs examined, 0.6 ± 1 structures present, and $*p < 1 \times 10^{-10}$, by a Student's *t* test) and *nhr-67(pf88)* animals with and without CKI-1::GFP ($n = 10$ ACs examined, 11 ± 2 structures present, $*p < 1 \times 10^{-7}$, by a Student's *t* test, and error bars represent SEM).

(C) Quantification of invadopodia number in mitotic ($n = 6$ mitotic ACs examined and 1.5 ± 1.6 structures present) and interphase ($n = 25$ interphase ACs examined, 0.8 ± 1.2 structures present, $p > 0.35$, by a Student's *t* test, and error bars represent SEM) following *nhr-67(RNAi)* treatment.

(D) DIC micrographs (left) and corresponding confocal sections of BM (laminin::GFP, second column) and F-actin (*cdh-3>mCherry::moesinABD*) (right). The F-actin was imaged ventrally (right) and the arrowheads indicate the position of the AC. The scale bars represent $5 \mu\text{m}$.

2010; Sela et al., 2012). Our data demonstrating that G1 arrest is required for the AC to express pro-invasive genes and to form invadopodia suggest that the invasive fate of the AC is a differentiated cellular state.

Differentiation of the Invasive Fate Is Dependent on the HDAC, HDA-1

Cellular differentiation requires changes in chromatin structure to regulate lineage specific gene expression programs (Li and Kirschner, 2014; Ma et al., 2015; Ruijtenberg and van den Heuvel, 2015; Singh et al., 2013). We thus reasoned that if invasive fate is a differentiated state, that the acquisition of this fate would require chromatin modifying genes. Therefore, we examined results from a whole genome RNAi screen (Matus et al., 2010). Notably, the HDAC, *hda-1*, whose vertebrate counterpart is an important regulator of differentiation (Chen et al., 2011; Ye et al., 2009), was required for AC invasion (Figure 5A) (Matus et al., 2010). Examination of a full-length *hda-1>HDA-1::GFP* expression reporter revealed that RNAi mediated loss of *nhr-67* resulted in a reduction of HDA-1::GFP expression in the AC (Figures 5B and 5C). These observations suggest that HDA-1 might be dependent on NHR-67 and function downstream of NHR-67 activity.

We next wanted to determine if HDA-1 functions downstream of NHR-67 to promote G1 arrest and whether it has a role in mediating the invasive fate. Loss of *hda-1* did not result in AC division (Table S3) or alter the localization of the G1 cell cycle marker CDT-1::GFP in the nucleus (Figure 5D; $n = 15/15$ animals). In addition, forced AC-specific expression of CKI-1 (to lock the AC in a G1 arrest state) failed to rescue AC invasion following *hda-1(RNAi)* treatment (Figure 5E). These results indicate that HDA-1 is not required for the AC to enter G1 arrest. We also found that early markers of AC fate (*cdh-3*, *pat-3*, and *lin-3*) were still expressed in the AC after RNAi mediated targeting of *hda-1* (Figures 6A and 6B) (Matus et al., 2010). Similar to loss of *nhr-67*, reduction of *hda-1* blocked acquisition of the AC invasive fate. RNAi targeting of *hda-1* resulted in a loss of invadopodia (Figures 6C and 6D) and a dramatic reduction in the expression of AC-expressed MMPs, hemiscentin, and actin regulators (Figures 6A and 6B). Taken together, the findings of NHR-67 regulation of HDA-1::GFP expression and similar phenotype of HDA-1 depletion to loss of *nhr-67*, suggests that HDA-1 functions downstream of *nhr-67* and G1 arrest to promote acquisition of the invasive fate. Importantly, however, we cannot rule out an independent function of HDA-1 acting in parallel to NHR-67 and G1 arrest in regulating AC differentiation.

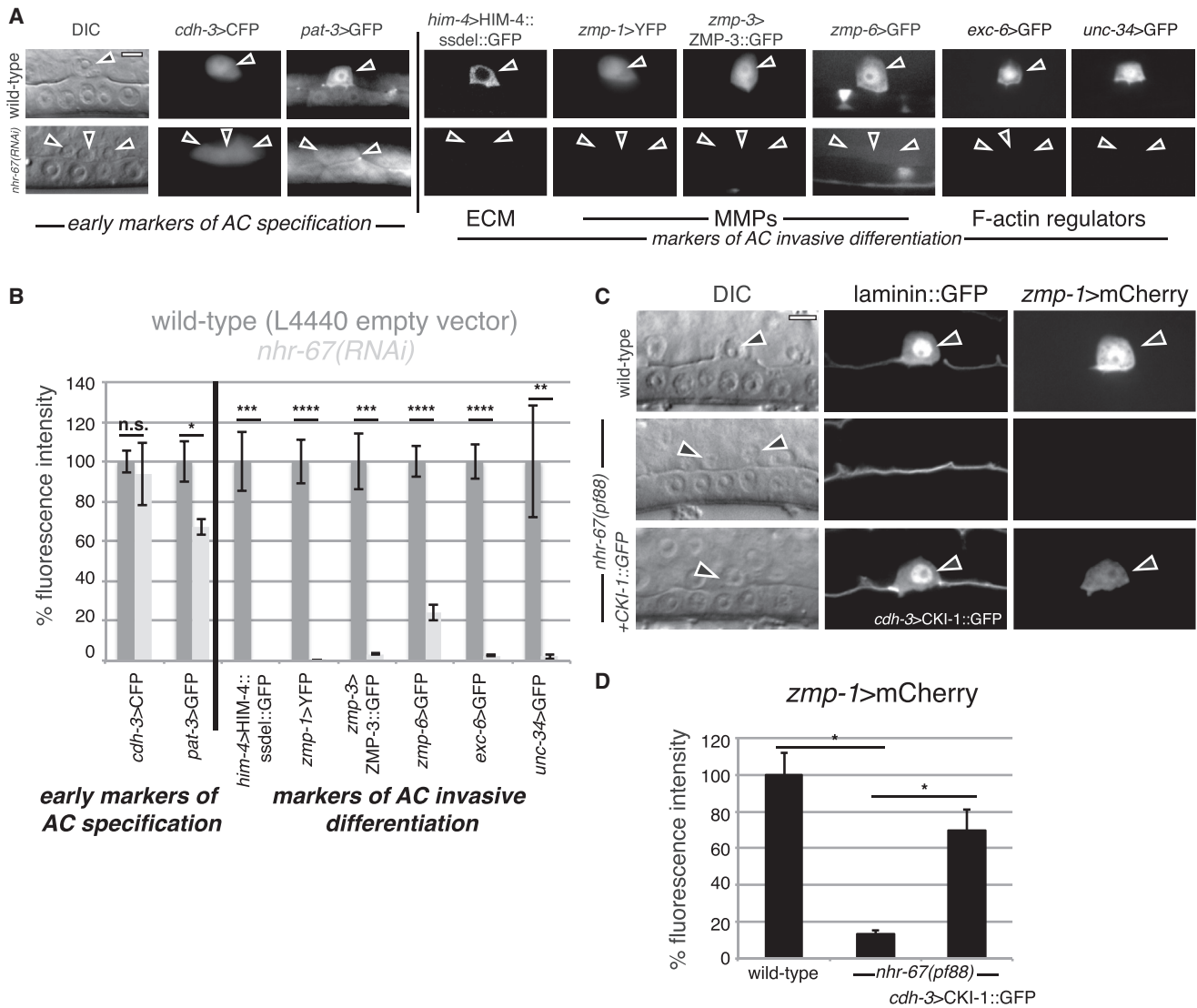


Figure 4. *nhr-67*-Deficient ACs Fail to Express Markers of Invasive Differentiation

(A) DIC images (left), corresponding fluorescence images of early markers of AC specification (*cdh-3>CFP* and *pat-3>GFP*), and later markers of invasive differentiation (*him-4>HIM-4::ssdel::GFP*, *zmp-1>YFP*, *zmp-3>ZMP-3::GFP*, *zmp-6>GFP*, *exc-6>GFP*, and *unc-34>GFP*) in wild-type (top) and *nhr-67(RNAi)*-treated animals with multiple ACs (bottom). The arrowheads indicate the position of the ACs.

(B) Quantification of fluorescence intensity comparing fluorescence reporters following *nhr-67(RNAi)* depletion ($n > 11$ animals examined for each; not significant, n.s.; $p > 0.7$; * $p < 0.01$; ** $p < 0.0001$; by a Student's t test; and error bars represent SEM).

(C) DIC micrographs (left) and corresponding confocal sections of the BM (laminin::GFP, middle) and *zmp-1>mCherry* (right) in wild-type (top), *nhr-67(pf88)* (middle), and *nhr-67(pf88); cdh-3>CKI-1::GFP* (bottom).

(D) Quantification of fluorescence intensity of *zmp-1>mCherry* in wild-type, *nhr-67(pf88)* animals with multiple ACs, and *nhr-67(pf88)* with CKI-1::GFP ($n > 13$ examined for each, * $p < 0.001$, by a Student's t test, and error bars represent SEM). The scale bars represent 5 μ m. See also Figure S3.

Induction of G1 Arrest Restores Invasion in Descendants of the AC

After loss of *nhr-67*, the dividing ACs continued to express early AC specification markers (see Figure 4A). This suggested that these dividing cells are an undifferentiated pool of pre-invasive cells with the potential to be invasive. If G1 arrest acts as a trigger for the differentiation of invasive fate, we hypothesized that restoration of G1 arrest following AC divisions should promote invasive fate differentiation. To test this notion, we induced *cki-1* expression using a heat-shock promoter after divisions of the AC had

initiated in *nhr-67* mutant animals. In all cases with detectable CKI-1::GFP in the ACs, we saw multiple ACs breaching the BM (Figure 6E; Table S3). We conclude that the dividing ACs in *nhr-67* mutants are an undifferentiated pre-invasive cell population, whose invasive fate can be realized by inducing G1 arrest.

DISCUSSION

We have found that the transcription factor NHR-67/TLX is a crucial regulator of the *C. elegans* AC invasion program. We

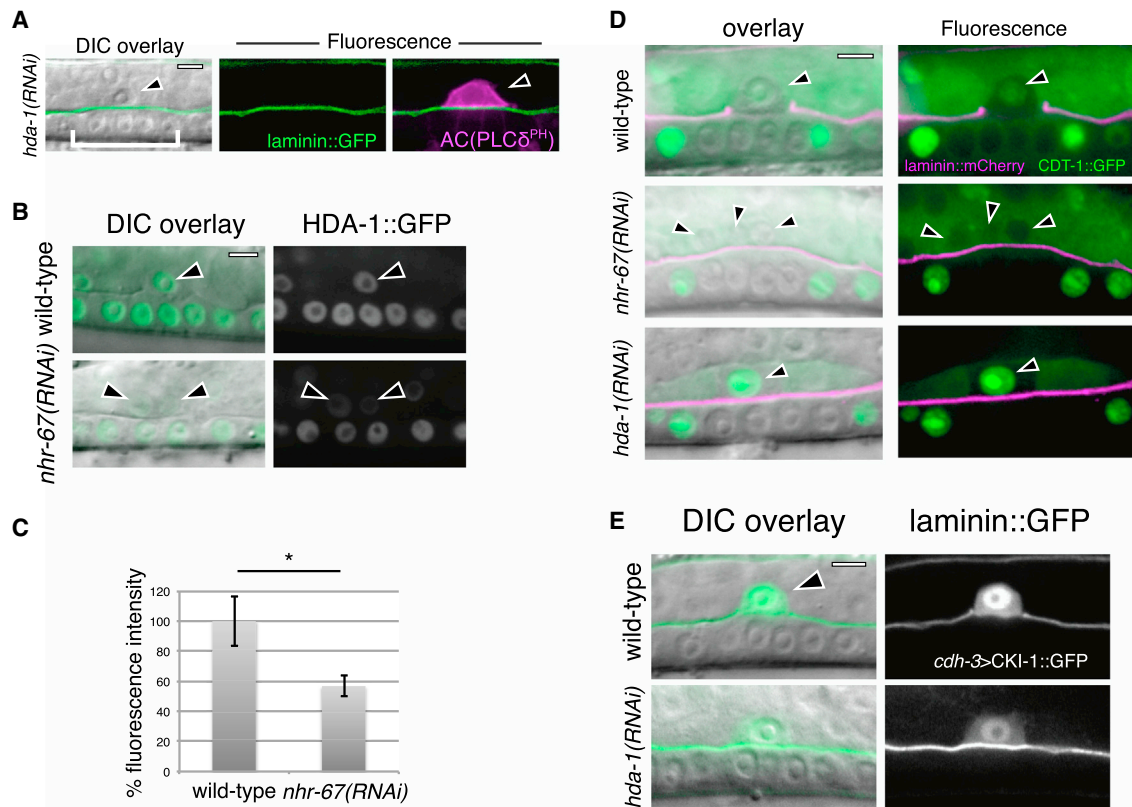


Figure 5. HDAC HDA-1 Expression Is Dependent on NHR-67 but Is Not Required for G1 Arrest

(A) DIC overlay (left) and fluorescence (middle, right) of AC invasion defect following *hda-1(RNAi)* depletion. The arrowheads indicate the position of the ACs. (B) DIC overlay (left) and GFP confocal images (right) of *hda-1>HDA-1::GFP* localization in wild-type (top) compared to *nhr-67(RNAi)* depletion. (C) Quantification of fluorescence intensity comparing *hda-1>HDA-1::GFP* following *nhr-67(RNAi)* depletion ($n > 10$ animals examined for each, * $p < 0.01$, by a Student's t test, and error bars represent SEM). (D) DIC overlay (left) and corresponding confocal images of laminin::mCherry (magenta) and *cdt-1>CDT-1::GFP* (green; right) of a wild-type animal (top), *nhr-67(RNAi)*-treated animal (middle), and *hda-1(RNAi)*-treated animal (bottom). (E) DIC overlay (left) and corresponding confocal images of laminin::GFP and *cdh-3>CKI-1::GFP* (right) in wild-type (top) and *hda-1(RNAi)*-depletion.

show that NHR-67 directs the AC into G1 cell-cycle arrest and that G1 arrest is specifically required for the AC to acquire the specialized features of an invasive cell, expression of MMPs and actin regulators as well as formation of invadopodia (Figure 6F). Our results further identify a requirement for the chromatin modifying HDAC HDA-1 functioning downstream or in parallel to NHR-67 and G1 arrest in promoting pro-invasive gene expression and invadopodia construction. Together these results offer compelling evidence that the AC invasive fate is a differentiated cellular state requiring G1 arrest and HDAC-dependent alterations in gene expression.

In the absence of NHR-67, we have found that the AC is initially specified correctly, but that it fails to enter G1 arrest and instead inappropriately enters the cell cycle and initiates divisions. Our data indicate that NHR-67 promotes G1 arrest in part through regulation of the cyclin-dependent kinase *cki-1*, as endogenous *cki-1* transcripts were dramatically decreased in the AC following NHR-67 depletion. Furthermore, restoration of *cki-1* in *nhr-67* mutants reestablished G1 arrest. The *cki-1* intergenic region contains multiple potential NHR-67 binding sites, consistent with the possibility that *cki-1* is a direct target of NHR-67. The only known direct target of NHR-67 in *C. elegans* is *cog-1*, an

Nkx6 homeodomain gene involved in left-right neuronal asymmetries. *cog-1* expression is regulated by NHR-67 through a single binding site (Sarin et al., 2009). Importantly, loss of *cki-1* resulted in only rare cases of dividing ACs, suggesting that redundant mechanisms regulate G1 arrest. This is consistent with observations in both *C. elegans* and *Drosophila* demonstrating that cells utilize a combination of CKI activity and other poorly understood mechanisms to trigger G1 cell-cycle arrest (Buttitta et al., 2007; Fay et al., 2002; Ruijtenberg and van den Heuvel, 2015).

A role for NHR-67 in regulating cell-cycle progression has not yet been demonstrated in other cells during *C. elegans* development. NHR-67 does, however, have a shared function in mediating cell fate determination in multiple cell types, including left/right asymmetric diversification of the gustatory ASE neuron (Sarin et al., 2009). NHR-67 and HDA-1 also promote distinct aspects of AC and neighboring VU cell differentiation, as both are required for the expression of the *lag-2/Delta* signal in the AC and the *lin-12/Notch* receptor in the VU cells (Ranawade et al., 2013; Verghese et al., 2011). Furthermore, NHR-67 mediates male linker cell migration, the male equivalent cell lineage of the hermaphrodite AC. Interestingly, similar to the AC, *nhr-67*

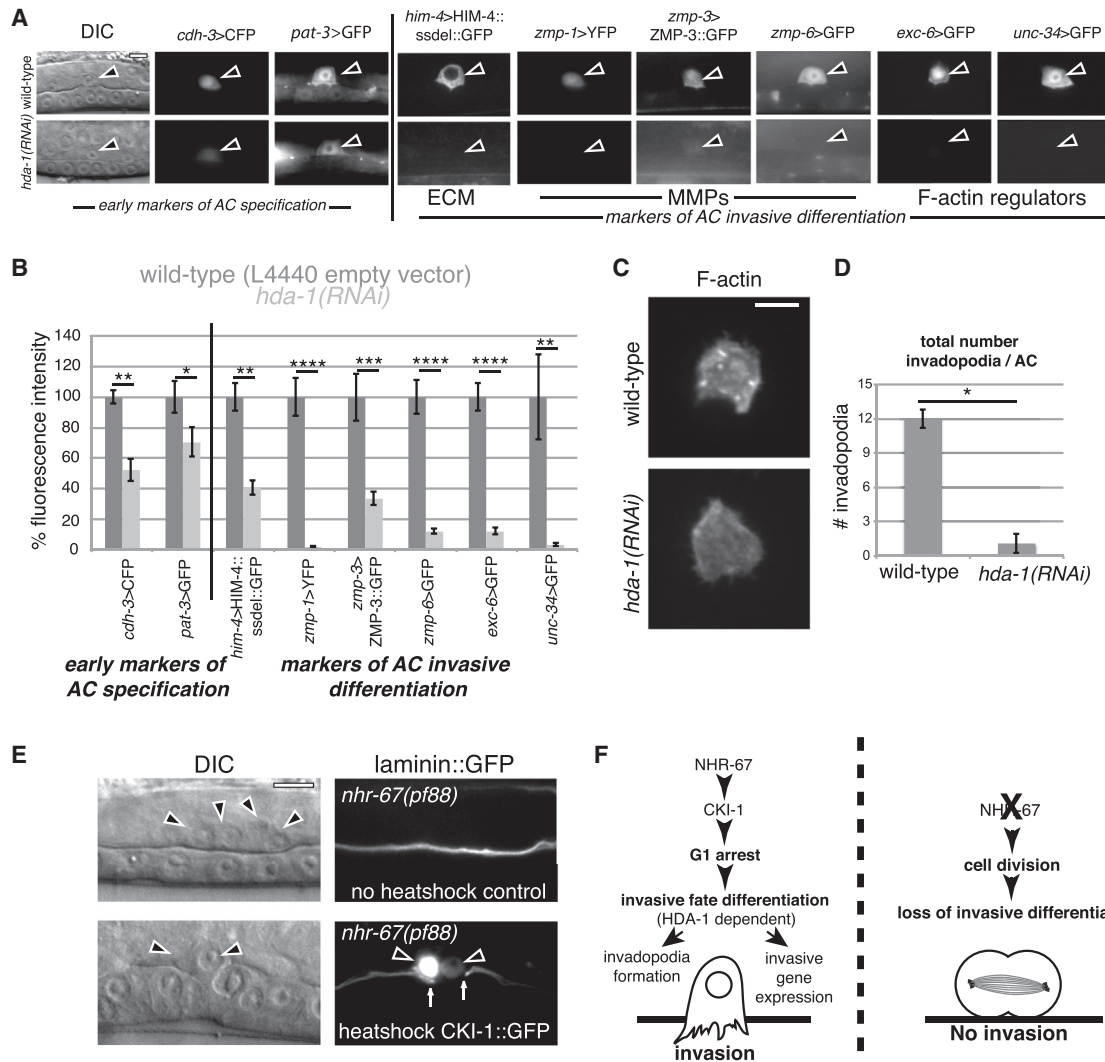


Figure 6. HDA-1 Is Required for Acquisition of the Invasive Fate

(A) DIC images (left), corresponding fluorescence images of early markers of AC specification (*cdh-3>CFP* and *pat-3>GFP*), and later markers of invasive differentiation (*him-4>HIM-4::ssdel::GFP*, *zmp-1>YFP*, *zmp-3>ZMP-3::GFP*, *zmp-6>GFP*, *exc-6>GFP*, and *unc-34>GFP*) in *hda-1(RNAi)*-treated animals (bottom).

(B) Quantification of fluorescence intensity comparing fluorescence reporters following *hda-1(RNAi)* depletion (n > 11 animals examined for each, *p < 0.05, **p < 0.01, ***p < 0.001, by a Student's t test, and error bars represent SEM).

(C) Ventral projection of confocal z stacks showing punctate F-actin-rich invadopodia along the basal surface of the AC in wild-type (top) and an *hda-1(RNAi)*-treated animal (bottom).

(D) Bar graph depicts quantification of invadopodia number in wild-type (n = 9 ACs examined and 12 ± 1 structures present) as compared to *hda-1(RNAi)*-treated animals (n = 10 ACs examined, 1 ± 0.5 structures present, *p < 3 × 10⁻⁶, by a Student's t test, and error bars represent SEM).

(E) DIC overlay (left) and confocal images (right) of an *nhr-67(pf88)* mutant (top) with multiple ACs and one at the (bottom) with induced expression of CKI-1::GFP after AC divisions showing multiple ACs breaching the BM (arrows).

(F) Summary model of NHR-67 and HDA-1 activity. The scale bars represent 5 μm.

also promotes the expression of the MMP *zmp-1* (Kato and Sternberg, 2009; Schwarz et al., 2012), but is not required to maintain the linker cell in a non-dividing state. A relationship between vertebrate NHR-67 orthologs and cell-cycle regulation does exist in vertebrate development and cancer progression. The *nhr-67* ortholog, TLX, likely through a conserved interaction with HDACs, maintains the proliferation of embryonic and adult neural stem cells (Park et al., 2010; Qu et al., 2010; Sun et al., 2007). TLX upregulation is also associated with triple negative

breast cancer and, intriguingly, functional studies have associated its activity with proliferation and invasion in vitro (Lin et al., 2015). Thus, NHR-67/TLX transcription factors may have a conserved role regulating cell proliferation as well as invasion in other contexts.

Although the AC was initially specified correctly after loss of *nhr-67*, the dividing descendants were incapable of invading through BM and initiating uterine-vulval connection. Previous studies have suggested that the cytoskeletal demands of

migratory and invasive cells may be incompatible with cell division (Qian et al., 2013; Vega et al., 2004). While our data do not rule out this possibility, blocking division by arresting the AC in the S or G2 phase did not rescue invasion in *nhr-67* mutants, indicating that competition for cytoskeletal elements is not sufficient to account for the incompatibility of invasion with division. Instead, our data demonstrate that G1 arrest is specifically required for invasion. NHR-67 activity appears to be only needed to maintain the AC in the G1 phase of the cell cycle, as AC-specific expression of CKI-1, which induces G1 arrest, completely rescued the invasive ability of the AC in the absence of *nhr-67*. It is well established that G1 arrest is strongly coupled with cellular differentiation during development (Buttitta et al., 2007; Sarkar et al., 2010; Sela et al., 2012). This suggests that G1 arrest in the AC might be required to fully acquire the invasive cell fate. Strongly supporting this notion, we show that G1 arrest is necessary for the AC to take on specialized characteristics of invasive cells, MMP, cell matrix, and actin regulator expression as well as invadopodia formation. Furthermore, we demonstrate that invasion can be restored by inducing CKI-1 expression in the dividing descendants of the AC in *nhr-67* mutants, strongly suggesting that these dividing ACs are an undifferentiated pool of pre-invasive cells capable of fully differentiating the invasive fate when the cells are placed in G1 arrest.

While observations from the last 30 years have suggested an association between the G1 phase of the cell cycle and differentiation (Gonzales et al., 2015; Jonk et al., 1992; Mummery et al., 1987; Ruijtenberg and van den Heuvel, 2015; Sela et al., 2012; Singh and Dalton, 2009), the molecular mechanisms that connect cell-cycle state and differentiation are poorly understood. Recent work has suggested that cell-cycle status might regulate chromatin structure to mediate cell fate decisions. Using the fluorescent ubiquitylation-based cell cycle indicator (FUCCI) system (Sakaue-Sawano et al., 2008) to examine cell-cycle regulation at single-cell resolution, Singh et al. (2013) found that human ES cells in the G1 phase are enriched for the expression of developmental regulatory genes. This cell-cycle-specific regulation of gene expression correlated with high levels of global 5-hydroxymethylcytosine (5hmC), an epigenetic modification that peaks in late G1 phase (Singh et al., 2013). Although the mechanism that links 5hmC modification to G1 arrest is unknown, cell-cycle regulation of 5hmC may have important roles in differentiation, as 5hmC is associated with active promoters and increased expression of differentiation genes (Ma et al., 2015; Pastor et al., 2011; Singh et al., 2013). Notably, our data indicate that the conserved HDAC, *hda-1*, a chromatin remodeling protein, is upregulated in the AC in response to G1 arrest and promotes acquisition of the invasive fate by regulating the expression of pro-invasive genes and the formation of invadopodia. HDACs are crucial mediators of cellular differentiation in multiple cell types, including oligodendrocytes (Ye et al., 2009), cardiomyocytes (Hoxha et al., 2012), and in the embryonic kidney (Chen et al., 2011). Although we cannot rule out the possibility that HDA-1 acts in parallel to NHR-67 and G1 arrest to mediate invasive fate, our observations are consistent with the idea that HDA-1 functions downstream of NHR-67 and G1 arrest and adds support to the idea that G1 arrest is linked to alterations in chromatin that promote cellular differentiation. In addition, as HDACs are strongly implicated in promoting invasion in numerous cancers

(Liu et al., 2003; McGarry et al., 2004; Park et al., 2011), our observations suggest that current treatments targeting HDACs (Liu et al., 2003; Minucci and Pelicci, 2006; Witt et al., 2009) might be particularly effective in halting invasion by broadly blocking the acquisition of invasive cell fate.

Invasive ability is correlated with decreased cell proliferation in cancer cell lines, tumor models, and human cancers (Gil-Henn et al., 2013; Hoek et al., 2008; Patsos et al., 2010; Rubio, 2008; Svensson et al., 2003; Wang et al., 2004). A few studies have also linked invasive ability specifically to G1 arrest using in vitro invasion assays (Baniwal et al., 2010; Qian et al., 2013; Yano et al., 2014). Furthermore, developmental EMT events, which require breaching BM, have been associated with the G1 phase of the cell cycle (Vega et al., 2004). These observations suggest that G1 arrest might be a common requirement to acquire the invasive cell fate. Interestingly, after G1 arrested neural crest cells complete EMT and delaminate from the neural tube, the cells enter S phase and proliferate (Burstyn-Cohen and Kalcheim, 2002). While the AC never divides following G1 arrest (it rapidly fuses with neighboring uterine cells following invasion, see Newman and Sternberg, 1996), a comparative study of uterine-vulval development in a distantly related nematode, *Panagrolaimus sp.* 1579, showed that when the AC is laser ablated prior to invasion, a neighboring VU cell can acquire AC fate, invade, and then divide (Félix and Sternberg, 1996). This suggests that G1 arrested invasive fate is a flexible arrest in many contexts that facilitates the invasion of founder cells into or out of a tissue, which can then shift to a proliferative state to generate additional cells and tissues. Given that most cytotoxic chemotherapy drugs do not target G1 arrested cancer cells (Yano et al., 2014), an important implication from these observations is that current therapeutic strategies would not target invading cells and might even select for more invasive tumors, as these invading cells may survive treatment, re-enter the cell cycle at a later time, and seed more aggressive tumors. Thus, effective therapeutic strategies may need to target both dividing cells and non-dividing invasive cells to halt metastasis.

EXPERIMENTAL PROCEDURES

C. elegans Culture Conditions

Rearing and handling of *C. elegans* was done using standard culture conditions at 15°C, 20°C, and 25°C as previously described (Brenner, 1974). Wild-type *C. elegans* animals were strain N2. In the text and figures, we designate linkage to a promoter with a greater than symbol (>) and use a double colon (::) for linkages that fuse open reading frames.

RNAi

We generated a set of 1,438 RNAi clones targeting an overlapping set of genes predicted to have transcription factor activity from the two commercially available genome-wide RNAi libraries, the *C. elegans* RNAi library (Source BioScience) (Kamath et al., 2003) and the *C. elegans* open reading frame (ORF)-RNAi library (Source BioScience) (Rual et al., 2004). Our combined transcription factor library targeted 86% (854) of the 988 transcription factors predicted in the *C. elegans* genome (see Table S1) (Haerty et al., 2008). RNAi feeding was performed following L1 synchronization by hypochlorite treatment. Uterine-specific RNAi sensitive L1 animals (*fos-1a>RDE-1*, *myo-2>YFP*; *rde-1(ne219)*; *rrf-3(pk1426)*) (Matus et al., 2010) were fed on bacterial lawns of *Escherichia coli* expressing double-stranded RNA for ~51 hr, in six-well plates, and screened for the presence of a Pvl phenotype using a dissecting microscope. There were 50–100 animals that were examined per well and the number of Pvl animals was recorded. All RNAi clones that resulted in the

presence of Pvl animals were re-screened (see Table S2). The empty RNAi vector, L4440, was used as a negative control and RNAi clones encoding *fos-1* and *mep-1*, two transcription factors known to produce Pvl phenotypes following RNAi knockdown (Matus et al., 2010; Sherwood et al., 2005), were used as positive controls.

Following the initial RNAi high-throughput screen, the RNAi vector encoding double-stranded RNA targeting *nhr-67* was sequenced to verify the correct insert. This *nhr-67* RNAi clone was then used in subsequent experiments and delivered by feeding to synchronized L1-arrested larvae. For experiments targeting *cdk-1*, the corresponding ORF-RNAi library clone (Rual et al., 2004) was delivered by feeding using the same methods as described above. A double-stranded (ds)RNA construct targeting the sole PCNA ortholog, *pcn-1*, was designed and cloned into L4440.

AC Invasion and Multiple AC Phenotype Scoring

AC invasion scoring was based upon the timing of the division of the underlying P6.p VPC as previously described (Matus et al., 2010; Sherwood and Sternberg, 2003). Briefly, at the P6.p one-cell stage (early L3), the VPCs (P5.p–P7.p) are separated from the uterine AC by the gonadal and epidermal BMs. At the P6.p two-cell stage (mid-L3 stage), the AC initiates invasion by breaching both BMs. AC invasion was scored at the P6.p four-cell stage (mid-to-late L3 stage) by examining the BM for a breach using either differential interference contrast (DIC) optics or laminin::GFP. The number of ACs was determined using early AC specification reporters including *lin-3>NLS::GFP*, *cdh-3^{1.5}>mCherry::PLC δ ^{PH}* or *cdh-3>mCherry::moesinABD*.

Statistical Analysis

Statistical analyses were performed using either a two-tailed unpaired Student's *t* test or a Fisher's exact probability test. Figure legends specify when each test was used.

SUPPLEMENTAL INFORMATION

Supplemental Information includes Supplemental Experimental Procedures, three figures, five tables, and one movie and can be found with this article online at <http://dx.doi.org/10.1016/j.devcel.2015.10.002>.

AUTHOR CONTRIBUTIONS

All authors designed the experiments. D.Q.M., A.J.S., L.L.L., A.Q.K., W.Z., Q.C., and M.B. performed the experiments. D.Q.M., L.C.K., L.L.L., and D.R.S. wrote the paper.

ACKNOWLEDGMENTS

We are grateful to M. Sarov for the *CKI-1::GFP* fosmid, K. Shen for the Q system vectors, H. Sawa and M. Krause for *cyd-1>GFP* and *cdk-4>GFP* vectors, A. Maddox for the *H2B::GFP* vector, S. Heuvel for *cki-1>CKI-1::GFP*, and B. Wightman for the *nhr-67(pf88)* allele. Some strains were provided by the Caenorhabditis Genetics Center (CGC), which is funded by NIH Office of Research Infrastructure Programs (P40 OD010440). We thank M. Morrissey for comments on the manuscript. This work was supported by grants from the NIH, the Pew Scholars Program in the Biomedical Sciences, the American Cancer Society, and the Leukemia and Lymphoma Society. D.Q.M. is supported by the Leukemia and Lymphoma Society (3601-11/388-0036) and the National Cancer Institute (4R00CA154870-03); A.J.S. is supported by the American Cancer Society; and L.C.K. and D.R.S. are supported by the National Institute of General Medical Sciences (F32GM103148 and GM079320).

Received: July 14, 2015

Revised: October 1, 2015

Accepted: October 2, 2015

Published: October 26, 2015

REFERENCES

Baniwal, S.K., Khalid, O., Gabet, Y., Shah, R.R., Purcell, D.J., Mav, D., Kohn-Gabet, A.E., Shi, Y., Coetzee, G.A., and Frenkel, B. (2010). Runx2 transcrip-

tone of prostate cancer cells: insights into invasiveness and bone metastasis. *Mol. Cancer* 9, 258.

Berthier-Vergnes, O., Kharbili, M.E., de la Fouchardière, A., Pointecouteau, T., Verrando, P., Wierinckx, A., Lachuer, J., Le Naour, F., and Lamartine, J. (2011). Gene expression profiles of human melanoma cells with different invasive potential reveal TSPAN8 as a novel mediator of invasion. *Br. J. Cancer* 104, 155–165.

Brenner, S. (1974). The genetics of *Caenorhabditis elegans*. *Genetics* 77, 71–94.

Burstyn-Cohen, T., and Kalcheim, C. (2002). Association between the cell cycle and neural crest delamination through specific regulation of G1/S transition. *Dev. Cell* 3, 383–395.

Buttitta, L.A., and Edgar, B.A. (2007). Mechanisms controlling cell cycle exit upon terminal differentiation. *Curr. Opin. Cell Biol.* 19, 697–704.

Buttitta, L.A., Katzaroff, A.J., Perez, C.L., de la Cruz, A., and Edgar, B.A. (2007). A double-assurance mechanism controls cell cycle exit upon terminal differentiation in *Drosophila*. *Dev. Cell* 12, 631–643.

Chen, S., Bellow, C., Yao, X., Stefkova, J., Dipp, S., Saifudeen, Z., Bachvarov, D., and El-Dahr, S.S. (2011). Histone deacetylase (HDAC) activity is critical for embryonic kidney gene expression, growth, and differentiation. *J. Biol. Chem.* 286, 32775–32789.

De Falco, G., Comes, F., and Simone, C. (2006). pRb: master of differentiation. Coupling irreversible cell cycle withdrawal with induction of muscle-specific transcription. *Oncogene* 25, 5244–5249.

de la Serna, I.L., Ohkawa, Y., and Imbalzano, A.N. (2006). Chromatin remodeling in mammalian differentiation: lessons from ATP-dependent remodelers. *Nat. Rev. Genet.* 7, 461–473.

Eckert, M.A., Lwin, T.M., Chang, A.T., Kim, J., Danis, E., Ohno-Machado, L., and Yang, J. (2011). Twist1-induced invadopodia formation promotes tumor metastasis. *Cancer Cell* 19, 372–386.

Fay, D.S., Keenan, S., and Han, M. (2002). *fzr-1* and *lin-35/Rb* function redundantly to control cell proliferation in *C. elegans* as revealed by a nonbiased synthetic screen. *Genes Dev.* 16, 503–517.

Félix, M.A., and Sternberg, P.W. (1996). Symmetry breakage in the development of one-armed gonads in nematodes. *Development* 122, 2129–2142.

Fujita, M., Takeshita, H., and Sawa, H. (2007). Cyclin E and CDK2 repress the terminal differentiation of quiescent cells after asymmetric division in *C. elegans*. *PLoS ONE* 2, e407.

Gil-Henn, H., Patsialou, A., Wang, Y., Warren, M.S., Condeelis, J.S., and Koleske, A.J. (2013). Arg/Abl2 promotes invasion and attenuates proliferation of breast cancer in vivo. *Oncogene* 32, 2622–2630.

Gonzales, K.A., Liang, H., Lim, Y.S., Chan, Y.S., Yeo, J.C., Tan, C.P., Gao, B., Le, B., Tan, Z.Y., Low, K.Y., et al. (2015). Deterministic restriction on pluripotent state dissolution by cell-cycle pathways. *Cell* 162, 564–579.

Gurskaya, N.G., Verkhusha, V.V., Shcheglov, A.S., Staroverov, D.B., Chepurnykh, T.V., Fradkov, A.F., Lukyanov, S., and Lukyanov, K.A. (2006). Engineering of a monomeric green-to-red photoactivatable fluorescent protein induced by blue light. *Nat. Biotechnol.* 24, 461–465.

Haerty, W., Artieri, C., Khezri, N., Singh, R.S., and Gupta, B.P. (2008). Comparative analysis of function and interaction of transcription factors in nematodes: extensive conservation of orthology coupled to rapid sequence evolution. *BMC Genomics* 9, 399.

Hagedorn, E.J., Yashiro, H., Ziel, J.W., Ihara, S., Wang, Z., and Sherwood, D.R. (2009). Integrin acts upstream of netrin signaling to regulate formation of the anchor cell's invasive membrane in *C. elegans*. *Dev. Cell* 17, 187–198.

Hagedorn, E.J., Ziel, J.W., Morrissey, M.A., Linden, L.M., Wang, Z., Chi, Q., Johnson, S.A., and Sherwood, D.R. (2013). The netrin receptor DCC focuses invadopodia-driven basement membrane transmigration in vivo. *J. Cell Biol.* 201, 903–913.

Hagedorn, E.J., Kelley, L.C., Naegeli, K.M., Wang, Z., Chi, Q., and Sherwood, D.R. (2014). ADF/cofilin promotes invadopodial membrane recycling during cell invasion in vivo. *J. Cell Biol.* 204, 1209–1218.

Hoek, K.S., Eichhoff, O.M., Schlegel, N.C., Döbbling, U., Kobert, N., Schaerer, L., Hemmi, S., and Dummer, R. (2008). In vivo switching of human

- melanoma cells between proliferative and invasive states. *Cancer Res.* **68**, 650–656.
- Hong, Y., Roy, R., and Ambros, V. (1998). Developmental regulation of a cyclin-dependent kinase inhibitor controls postembryonic cell cycle progression in *Caenorhabditis elegans*. *Development* **125**, 3585–3597.
- Hoxha, E., Lambers, E., Xie, H., De Andrade, A., Krishnamurthy, P., Wasserstrom, J.A., Ramirez, V., Thal, M., Verma, S.K., Soares, M.B., and Kishore, R. (2012). Histone deacetylase 1 deficiency impairs differentiation and electrophysiological properties of cardiomyocytes derived from induced pluripotent cells. *Stem Cells* **30**, 2412–2422.
- Jonk, L.J., de Jonge, M.E., Kruyt, F.A., Mummery, C.L., van der Saag, P.T., and Kruijjer, W. (1992). Aggregation and cell cycle dependent retinoic acid receptor mRNA expression in P19 embryonal carcinoma cells. *Mech. Dev.* **36**, 165–172.
- Kamath, R.S., Fraser, A.G., Dong, Y., Poulin, G., Durbin, R., Gotta, M., Kanapin, A., Le Bot, N., Moreno, S., Sohrmann, M., et al. (2003). Systematic functional analysis of the *Caenorhabditis elegans* genome using RNAi. *Nature* **421**, 231–237.
- Kato, M., and Sternberg, P.W. (2009). The *C. elegans* *tailless/TLX* homolog *nhr-67* regulates a stage-specific program of linker cell migration in male gonadogenesis. *Development* **136**, 3907–3915.
- Kelley, L.C., Lohmer, L.L., Hagedorn, E.J., and Sherwood, D.R. (2014). Traversing the basement membrane in vivo: a diversity of strategies. *J. Cell Biol.* **204**, 291–302.
- Kim, Y., and Kipreos, E.T. (2007). The *Caenorhabditis elegans* replication licensing factor CDT-1 is targeted for degradation by the CUL-4/DDB-1 complex. *Mol. Cell Biol.* **27**, 1394–1406.
- Kimble, J., and Hirsh, D. (1979). The postembryonic cell lineages of the hermaphrodite and male gonads in *Caenorhabditis elegans*. *Dev. Biol.* **70**, 396–417.
- Li, V.C., and Kirschner, M.W. (2014). Molecular ties between the cell cycle and differentiation in embryonic stem cells. *Proc. Natl. Acad. Sci. USA* **111**, 9503–9508.
- Li, Z., Xu, Y., Zhang, C., Liu, X., Jiang, L., and Chen, F. (2014). Mammalian diaphanous-related formin 1 is required for motility and invadopodia formation in human U87 glioblastoma cells. *Int. J. Mol. Med.* **33**, 383–391.
- Lin, M.L., Patel, H., Remenyi, J., Banerji, C.R., Lai, C.F., Periyasamy, M., Lombardo, Y., Busonero, C., Ottaviani, S., Passey, A., et al. (2015). Expression profiling of nuclear receptors in breast cancer identifies TLX as a mediator of growth and invasion in triple-negative breast cancer. *Oncotarget* **6**, 21685–21703.
- Liu, L.T., Chang, H.C., Chiang, L.C., and Hung, W.C. (2003). Histone deacetylase inhibitor up-regulates RECK to inhibit MMP-2 activation and cancer cell invasion. *Cancer Res.* **63**, 3069–3072.
- Ma, Y., Kanakousaki, K., and Buttitta, L. (2015). How the cell cycle impacts chromatin architecture and influences cell fate. *Front. Genet.* **6**, 19.
- Matus, D.Q., Li, X.Y., Durbin, S., Agarwal, D., Chi, Q., Weiss, S.J., and Sherwood, D.R. (2010). In vivo identification of regulators of cell invasion across basement membranes. *Sci. Signal.* **3**, ra35.
- Matus, D.Q., Chang, E., Makohon-Moore, S.C., Hagedorn, M.A., Chi, Q., and Sherwood, D.R. (2014). Cell division and targeted cell cycle arrest opens and stabilizes basement membrane gaps. *Nat. Commun.* **5**, 4184.
- McGarry, L.C., Winnie, J.N., and Ozanne, B.W. (2004). Invasion of v-Fos(FBR)-transformed cells is dependent upon histone deacetylase activity and suppression of histone deacetylase regulated genes. *Oncogene* **23**, 5284–5292.
- Minucci, S., and Pelicci, P.G. (2006). Histone deacetylase inhibitors and the promise of epigenetic (and more) treatments for cancer. *Nat. Rev. Cancer* **6**, 38–51.
- Morrissey, M.A., Keeley, D.P., Hagedorn, E.J., McClatchey, S.T., Chi, Q., Hall, D.H., and Sherwood, D.R. (2014). B-LINK: a hemocentin, plakins, and integrin-dependent adhesion system that links tissues by connecting adjacent basement membranes. *Dev. Cell* **31**, 319–331.
- Mummery, C.L., van Rooijen, M.A., van den Brink, S.E., and de Laat, S.W. (1987). Cell cycle analysis during retinoic acid induced differentiation of a human embryonal carcinoma-derived cell line. *Cell Differ.* **20**, 153–160.
- Newman, A.P., and Sternberg, P.W. (1996). Coordinated morphogenesis of epithelia during development of the *Caenorhabditis elegans* uterine-vulval connection. *Proc. Natl. Acad. Sci. USA* **93**, 9329–9333.
- Nusser-Stein, S., Beyer, A., Rimann, I., Adamczyk, M., Piterman, N., Hajnal, A., and Fisher, J. (2012). Cell-cycle regulation of NOTCH signaling during *C. elegans* vulval development. *Mol. Syst. Biol.* **8**, 618.
- Ozanne, B.W., Spence, H.J., McGarry, L.C., and Hennigan, R.F. (2006). Invasion is a genetic program regulated by transcription factors. *Curr. Opin. Genet. Dev.* **16**, 65–70.
- Page-McCaw, A., Ewald, A.J., and Werb, Z. (2007). Matrix metalloproteinases and the regulation of tissue remodelling. *Nat. Rev. Mol. Cell Biol.* **8**, 221–233.
- Park, M., and Krause, M.W. (1999). Regulation of postembryonic G(1) cell cycle progression in *Caenorhabditis elegans* by a cyclin D/CDK-like complex. *Development* **126**, 4849–4860.
- Park, H.J., Kim, J.K., Jeon, H.M., Oh, S.Y., Kim, S.H., Nam, D.H., Kim, H., Nam, D.H., and Kim, H. (2010). The neural stem cell fate determinant TLX promotes tumorigenesis and genesis of cells resembling glioma stem cells. *Mol. Cells* **30**, 403–408.
- Park, S.Y., Jun, J.A., Jeong, K.J., Heo, H.J., Sohn, J.S., Lee, H.Y., Park, C.G., and Kang, J. (2011). Histone deacetylases 1, 6 and 8 are critical for invasion in breast cancer. *Oncol. Rep.* **25**, 1677–1681.
- Pastor, W.A., Pape, U.J., Huang, Y., Henderson, H.R., Lister, R., Ko, M., McLoughlin, E.M., Brudno, Y., Mahapatra, S., Kapranov, P., et al. (2011). Genome-wide mapping of 5-hydroxymethylcytosine in embryonic stem cells. *Nature* **473**, 394–397.
- Patsos, G., Germann, A., Gebert, J., and Dihlmann, S. (2010). Restoration of absent in melanoma 2 (AIM2) induces G2/M cell cycle arrest and promotes invasion of colorectal cancer cells. *Int. J. Cancer* **126**, 1838–1849.
- Qian, X., Hulit, J., Suyama, K., Eugenin, E.A., Belbin, T.J., Loudig, O., Smirnova, T., Zhou, Z.N., Segall, J., Locker, J., et al. (2013). p21CIP1 mediates reciprocal switching between proliferation and invasion during metastasis. *Oncogene* **32**, 2292–2303, 2303.e1–2303.e7.
- Qu, Q., Sun, G., Li, W., Yang, S., Ye, P., Zhao, C., Yu, R.T., Gage, F.H., Evans, R.M., and Shi, Y. (2010). Orphan nuclear receptor TLX activates Wnt/beta-catenin signalling to stimulate neural stem cell proliferation and self-renewal. *Nat. Cell Biol.* **12**, 31–40, 1–9.
- Ranawade, A.V., Cumbo, P., and Gupta, B.P. (2013). *Caenorhabditis elegans* histone deacetylase *hda-1* is required for morphogenesis of the vulva and LIN-12/Notch-mediated specification of uterine cell fates. *G3 (Bethesda)* **3**, 1363–1374.
- Ridenour, D.A., McLennan, R., Teddy, J.M., Semerad, C.L., Haug, J.S., and Kulesa, P.M. (2014). The neural crest cell cycle is related to phases of migration in the head. *Development* **141**, 1095–1103.
- Rowe, R.G., and Weiss, S.J. (2008). Breaching the basement membrane: who, when and how? *Trends Cell Biol.* **18**, 560–574.
- Rual, J.F., Ceron, J., Koreth, J., Hao, T., Nicot, A.S., Hirozane-Kishikawa, T., Vandenhaute, J., Orkin, S.H., Hill, D.E., van den Heuvel, S., and Vidal, M. (2004). Toward improving *Caenorhabditis elegans* phenome mapping with an ORFeome-based RNAi library. *Genome Res.* **14** (10B), 2162–2168.
- Rubio, C.A. (2008). Arrest of cell proliferation in budding tumor cells ahead of the invading edge of colonic carcinomas. A preliminary report. *Anticancer Res.* **28** (4C), 2417–2420.
- Ruijtenberg, S., and van den Heuvel, S. (2015). G1/S inhibitors and the SWI/SNF complex control cell-cycle exit during muscle differentiation. *Cell* **162**, 300–313.
- Sakaue-Sawano, A., Kurokawa, H., Morimura, T., Hanyu, A., Hama, H., Osawa, H., Kashiwagi, S., Fukami, K., Miyata, T., Miyoshi, H., et al. (2008). Visualizing spatiotemporal dynamics of multicellular cell-cycle progression. *Cell* **132**, 487–498.
- Sarin, S., Antonio, C., Tursun, B., and Hobert, O. (2009). The *C. elegans* *Tailless/TLX* transcription factor *nhr-67* controls neuronal identity and left/right asymmetric fate diversification. *Development* **136**, 2933–2944.

- Sarkar, S., Dey, B.K., and Dutta, A. (2010). MiR-322/424 and -503 are induced during muscle differentiation and promote cell cycle quiescence and differentiation by down-regulation of Cdc25A. *Mol. Biol. Cell* *21*, 2138–2149.
- Schwarz, E.M., Kato, M., and Sternberg, P.W. (2012). Functional transcriptomics of a migrating cell in *Caenorhabditis elegans*. *Proc. Natl. Acad. Sci. USA* *109*, 16246–16251.
- Sela, Y., Molotski, N., Golan, S., Itskovitz-Eldor, J., and Soen, Y. (2012). Human embryonic stem cells exhibit increased propensity to differentiate during the G1 phase prior to phosphorylation of retinoblastoma protein. *Stem Cells* *30*, 1097–1108.
- Sherwood, D.R., and Sternberg, P.W. (2003). Anchor cell invasion into the vulval epithelium in *C. elegans*. *Dev. Cell* *5*, 21–31.
- Sherwood, D.R., Butler, J.A., Kramer, J.M., and Sternberg, P.W. (2005). FOS-1 promotes basement-membrane removal during anchor-cell invasion in *C. elegans*. *Cell* *121*, 951–962.
- Singh, A.M., and Dalton, S. (2009). The cell cycle and Myc intersect with mechanisms that regulate pluripotency and reprogramming. *Cell Stem Cell* *5*, 141–149.
- Singh, A.M., Chappell, J., Trost, R., Lin, L., Wang, T., Tang, J., Matlock, B.K., Weller, K.P., Wu, H., Zhao, S., et al. (2013). Cell-cycle control of developmentally regulated transcription factors accounts for heterogeneity in human pluripotent cells. *Stem Cell Reports* *1*, 532–544.
- Sonneville, R., Craig, G., Labib, K., Gartner, A., and Blow, J.J. (2015). Both chromosome decondensation and condensation are dependent on DNA replication in *C. elegans* embryos. *Cell Rep.* *12*, 405–417.
- Sun, G., Yu, R.T., Evans, R.M., and Shi, Y. (2007). Orphan nuclear receptor TLX recruits histone deacetylases to repress transcription and regulate neural stem cell proliferation. *Proc. Natl. Acad. Sci. USA* *104*, 15282–15287.
- Svensson, S., Nilsson, K., Ringberg, A., and Landberg, G. (2003). Invade or proliferate? Two contrasting events in malignant behavior governed by p16(INK4a) and an intact Rb pathway illustrated by a model system of basal cell carcinoma. *Cancer Res.* *63*, 1737–1742.
- Valastyan, S., and Weinberg, R.A. (2011). Tumor metastasis: molecular insights and evolving paradigms. *Cell* *147*, 275–292.
- Vega, S., Morales, A.V., Ocaña, O.H., Valdés, F., Fabregat, I., and Nieto, M.A. (2004). Snail blocks the cell cycle and confers resistance to cell death. *Genes Dev.* *18*, 1131–1143.
- Vergheze, E., Schocken, J., Jacob, S., Wimer, A.M., Royce, R., Nesmith, J.E., Baer, G.M., Clever, S., McCain, E., Lakowski, B., and Wightman, B. (2011). The tailless ortholog nhr-67 functions in the development of the *C. elegans* ventral uterus. *Dev. Biol.* *356*, 516–528.
- Vlach, J., Hennecke, S., and Amati, B. (1997). Phosphorylation-dependent degradation of the cyclin-dependent kinase inhibitor p27. *EMBO J.* *16*, 5334–5344.
- Wang, W., Goswami, S., Lapidus, K., Wells, A.L., Wyckoff, J.B., Sahai, E., Singer, R.H., Segall, J.E., and Condeelis, J.S. (2004). Identification and testing of a gene expression signature of invasive carcinoma cells within primary mammary tumors. *Cancer Res.* *64*, 8585–8594.
- Wang, Z., Chi, Q., and Sherwood, D.R. (2014). MIG-10 (lamellipodin) has netrin-independent functions and is a FOS-1A transcriptional target during anchor cell invasion in *C. elegans*. *Development* *141*, 1342–1353.
- Wei, X., Potter, C.J., Luo, L., and Shen, K. (2012). Controlling gene expression with the Q repressible binary expression system in *Caenorhabditis elegans*. *Nat. Methods* *9*, 391–395.
- Witt, O., Deubzer, H.E., Milde, T., and Oehme, I. (2009). HDAC family: What are the cancer relevant targets? *Cancer Lett.* *277*, 8–21.
- Yano, S., Miwa, S., Mii, S., Hiroshima, Y., Uehara, F., Yamamoto, M., Kishimoto, H., Tazawa, H., Bouvet, M., Fujiwara, T., and Hoffman, R.M. (2014). Invading cancer cells are predominantly in G0/G1 resulting in chemoresistance demonstrated by real-time Fucci imaging. *Cell Cycle* *13*, 953–960.
- Ye, F., Chen, Y., Hoang, T., Montgomery, R.L., Zhao, X.H., Bu, H., Hu, T., Taketo, M.M., van Es, J.H., Clevers, H., et al. (2009). HDAC1 and HDAC2 regulate oligodendrocyte differentiation by disrupting the beta-catenin-TCF interaction. *Nat. Neurosci.* *12*, 829–838.
- Yuzyuk, T., Fakhouri, T.H., Kiefer, J., and Mango, S.E. (2009). The polycomb complex protein mes-2/E(z) promotes the transition from developmental plasticity to differentiation in *C. elegans* embryos. *Dev. Cell* *16*, 699–710.
- Ziel, J.W., Hagedorn, E.J., Audhya, A., and Sherwood, D.R. (2009). UNC-6 (netrin) orients the invasive membrane of the anchor cell in *C. elegans*. *Nat. Cell Biol.* *11*, 183–189.

Developmental Cell

Supplemental Information

**Invasive Cell Fate Requires G1 Cell-Cycle Arrest
and Histone Deacetylase-Mediated Changes
in Gene Expression**

David Q. Matus, Lauren L. Lohmer, Laura C. Kelley, Adam J. Schindler, Abraham Q. Kohrman, Michalis Barkoulas, Wan Zhang, Qiuyi Chi, and David R. Sherwood

Supplemental Experimental Procedures

C. elegans strains

The following alleles and transgenes were used in this study: *bmdEx1[cdh-3>CKI-1^{CK-}::GFP; myo-2>mCherry]*, *otEx3362[nhr-67>NHR-67::mCherry, elt-2::GFP]*, *qyEx258[unc-34>GFP]*, *maIs103[rnr-1>GFP]*, *qyIs92[hda-1>HDA-1::GFP]*, *qyIs193[cyd-1>GFP]*, *qyIs196[cdk-4>GFP]*, *qyIs225[cdh-3>mCherry::moeABD]*, *qyIs227[cdh-3>mCherry::moeABD]*, *qyIs229[cdh-3>H2B::GFP]*, *qyIs232[cdt-1>CDT-1::GFP]*, *qyIs270[cdh-3>H2B::dendra]*, *qyIs275[hsp-16-41>cki-1::GFP; myo-2>mCherry]*, *qyIs200[zmp-3>ZMP-3::GFP]*, *qyIs192[zmp-6>GFP]*, *qyIs301[pat-3>GFP]*, *qyIs185[exc-6>GFP]*, *qyIs347[cdh-3>QS::SL2::mCherry, cdh-3>QF::SL2::mCherry]*, *syIs129[him-4>HIM-4^{ssdel}::GFP]*; LGII, *osIs1[cye-1>CYE-1::GFP]*; *qyIs17[zmp-1>mCherry]*, *qyIs23[cdh-3^{1.5}>mCherry::PLCδ^{PH}]*, *rrf-3(pk1426)*, *syIs77[zmp-1>YFP]*; LGIII, *rde-1(ne219)*; LGIV, *nhr-67(pf88)*, *nhr-67(ok631)*, *syIs107[lin-3>NLS-GFP]*; *qyIs10[laminin::GFP]*; LGV, *qyIs266[cdh-3>cki-1::GFP]*, *syIs51[cdh-3>CFP]*; LGX *qyIs7[laminin::GFP]*, *qyIs24[cdh-3^{1.5}>mCherry::PLCδ^{PH}]*, *qyIs349[QUAS>nhr-67::venus, myo-2>mCherry]*.

Construction of GFP and mCherry protein fusions

The open reading frame of *nhr-67* was amplified from the ORF-RNAi library (Source BioScience, Nottingham, UK) (Rual, 2004) and cloned into the *NheI* and *XhoI* sites of the plasmid XW12 (gift of K. Shen, Stanford University). QS::SL2::mCherry and QF::SL2::mCherry were amplified from XW09 and XW17 (gift of K. Shen, Stanford University) (Wei et al., 2012) and *mCherry::moesinABD* was amplified from the plasmid

JWZ6. These PCR products were linked by PCR fusion to a 5 kb 5' cis-regulatory element of the *cdh-3* promoter, amplified from plasmid JP38, that drives AC-specific expression (Kirouac and Sternberg, 2003). A 5.4 kb fragment containing the entire *zmp-3* genomic region prior to its stop codon was amplified from N2 genomic DNA and then linked to GFP amplified from pPD95.75 by PCR fusion. A 7.8 kb fragment of the *zmp-6* promoter was amplified from N2 genomic DNA and then linked to GFP amplified from pPD95.75 by PCR fusion. Constructs were coinjected with 50 ng/ μ l *unc-119* rescue DNA, ~50ng/ μ l pBsSK, and 25 ng/ μ l EcoRI cut salmon sperm DNA into *unc-119(ed4)* hermaphrodites. Multiple stably expressing extrachromosomal lines were established and selected lines were integrated by gamma irradiation as previously described (Sherwood et al., 2005). See Tables S4 and S5 for transgenic strains generated and primer sequences used.

Construction of CKI-1^{CK-}::GFP

CKI-1::GFP was amplified from the fosmid WRM0626bF02 (gift of M. Sarov, Max Planck Institute, Dresden, Germany) and cloned into HindIII and NotI sites of the plasmid pcr2.1 (Life Technologies). Two rounds of site-directed mutagenesis were performed to induce four alanine substitutions, replacing arginine 6, leucine 8 and phenylalanines 41 and 43 in the N-terminal cdk/cyclin-binding region, which is conserved in metazoan cdk inhibitors and required to inhibit cyclin-dependent kinase activity to generate CKI-1^{CK-}::GFP (Vlach et al., 1997). This construct was linked by PCR fusion to a 5 kb 5' cis-regulatory element of the *cdh-3* promoter that drives AC-specific expression (Kirouac and Sternberg, 2003). *cdh-3*>CKI-1^{CK-1}::GFP; *nhr-67(pf88)*

animals were generated by co-injection of PCR fusion product and a HygR construct (*rps-0>hygR*, amplified from pDD205, gift of Dan Dickinson, University of North Carolina at Chapel Hill) for selection of extrachromosomal array lines using hygromycin resistance (Greiss and Chin, 2011).

Optical highlighting (photoconversion) to lineage AC fate

Single AC nuclei expressing *H2B::dendra* were photoconverted on an epifluorescence compound microscope (Axioimager, Carl Zeiss) equipped with a 100X objective excited using UV light for 10s. After photoconversion images were captured using a spinning disc confocal or an Axioimager microscope (Carl Zeiss). Animals were recovered from the agar pad and allowed to develop at 25°C for ~6-8 h and then reimaged.

Cell ablations

Laser-directed ablations of the AC were carried out on 5% agar pads as previously described (Sherwood and Sternberg, 2003). The AC was ablated at the early L3 stage (P6.p one-cell stage) in *nhr-67(RNAi)* treated uterine-specific RNAi sensitive animals (*fos-1a>RDE-1, myo-2>YFP; rde-1(ne219); rrf-3(pk1426)* (Matus et al., 2010)) expressing a marker of early AC-specification (*lin-3>NLS-GFP*). Ablated animals were recovered from the agar pad and left to develop at 25°C and then examined ~4 h later during the mid-to-late L3 stage (the time of normal AC invasion, P6.p four-cell stage) for the number of GFP positive ACs as indicated (see Figure S2).

Gene expression induction using the Q system and quinic acid desuppression treatment

To induce expression of *NHR-67::venus*, we created transgenic animals bearing *QUAS>NHR-67::venus* (*qyIs347*) crossed to a strain expressing *laminin::GFP* (*qyIs8*). AC-specific expression of the *QUAS* driven construct was generated by creating transgenic animals expressing *cdh-3>QS::SL2::mCherry* (repressor) and *cdh-3>QF::SL2::mCherry* (activator) (*qyIs349*). These animals were crossed together to generate a strain containing *laminin::GFP*, *QUAS>NHR-67::GFP*, and the AC-specific repressor and activator constructs that comprise the Q system. Quinic acid treatment was performed with the following modifications to the original protocol (Wei et al., 2012). Synchronized L1-arrested larvae were grown for 26.5 h at 25°C on regular NGM plates seeded with OP50 bacteria. At 26.5 h early L3 stage animals (P6.p one-cell stage) were transferred to NGM plates seeded with OP50 bacteria containing 300 µl quinic acid solution, ~40 µl 10N NaOH (for pH 6-7) and 40 µl M9. Induced expression of *nhr-67::venus* was detected in the AC using an Axioimager with a 100X objective 6-8h later during the mid-to-late L3 stage (the time of normal AC invasion, P6.p four-cell stage).

Heat shock CKI-1::GFP experiment

Synchronized starved L1 *nhr-67(pf88)* larvae containing an integrated *hsp16-41>cki-1::GFP* array (*qyIs275*) were plated on NGM plates with OP50 and allowed to develop at 25°C for 26 h until the early L3 stage (P6.p one-cell stage). High levels of CKI-1::GFP were induced with a 2h heat shock at 33°C and then animals were allowed to recover for 2 h. Animals were imaged 2-4 h later at the mid-to-late L3 stage (P6.p four-cell stage) on

a spinning disc confocal using a 100X objective and examined for invasion (using laminin::GFP (*qyIs7*)).

Induction of S- and G2-phase arrest in the AC

Synchronized starved L1 *nhr-67(pf88)* larvae containing an AC-specific reporter, *cdh-3>mCherry::moesinABD (qyIs227)* were plated on NGM plates with OP50 and allowed to develop at 25°C for 26 h until the early L3 stage (P6.p one-cell stage). To induce S-phase arrest animals were transferred to NGM plates seeded with OP50 containing 40mM hydroxyurea (Sigma). Feeding RNAi targeting the PCNA ortholog *pcn-1* and *cdk-1* were used to induce S- and G2-phase arrest. Animals were imaged at the mid-to-late L3 stage (P6.p four-cell stage) on a spinning disc confocal using a 100X objective to confirm cell-cycle arrest and examine BM invasion (using laminin::GFP (*qyIs7*)).

Data analysis

For scoring AC invasion, individual data points for each experiment were collected over multiple days. For those experiments that included RNAi knockdown, scoring data represents multiple RNAi treatments. For each experimental condition, no images that corresponded to the correct state were excluded from our analyses. Quantitative analyses of fluorescent reporters was performed in Image J. Images were first subjected to background subtraction using default parameters. Mean fluorescence intensity was calculated by applying a threshold and then using the wand tool to select the area of the AC. For images with signal too low to detect by applying a threshold, a DIC and fluorescence image overlay was created using the merge channels function and the area

of the AC was drawn using the freehand selection tool based off of the corresponding DIC image. Figures and graphs were constructed in Excel (Microsoft), Adobe Photoshop and Illustrator (CC; Adobe).

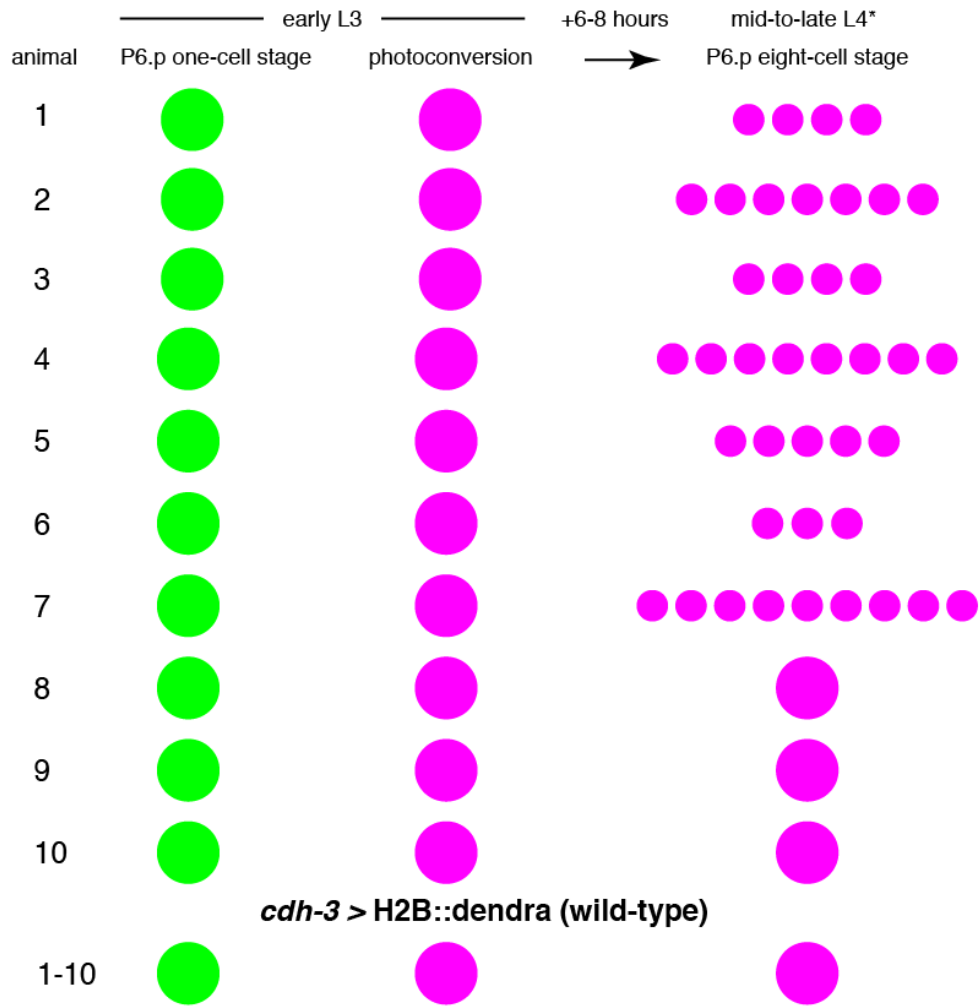
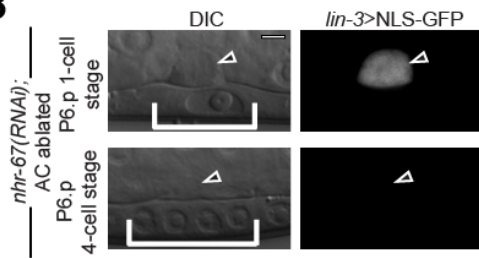
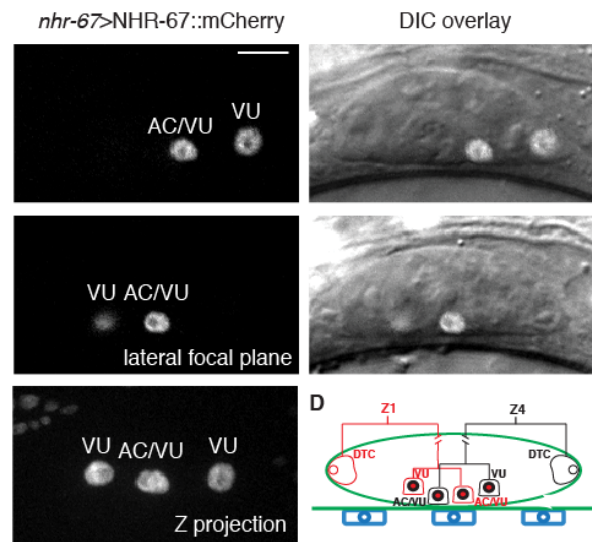
A*nhr-67(pf88); cdh-3 > H2B::dendra** all *cdh-3 > H2B::dendra* expressing ACs emitted fluorescence in 488 and 561 nm**B****C**

Figure S1. Lineage tracing and laser-directed ablation reveal that multiple ACs arise from a single AC after loss of *nhr-67(pf88)*. Related to Figure 1. (A) Chart depicts the number of ACs present (magenta, right) following optical highlighting in the *nhr-67(pf88)* hypomorph at the early L3 when only a single AC was present. Photocoverion of wild-type ACs resulted in the presence of a single AC (n = 10/10 animals). (B) DIC images (left) and corresponding fluorescence images (right) viewing the AC (arrowheads, expressing an early marker of AC-specification, *lin-3>NLS-GFP*) showing animal before laser-directed cell ablation (P6.p 1-cell stage, top) and 4 h later (P6.p 4-cell stage, bottom) after laser ablation (n = 3/3 animals examined with no GFP expression in the ventral uterus following laser ablation). White brackets indicate position of the primary VPCs. (C) *nhr-67* is expressed in the VU cells. Single plane of confocal z-stack (left) and DIC images with fluorescence overlay (right) depicts nuclear localization of *nhr-67>NHR-67::mCherry* in two lateral focal planes (top, middle). Maximum intensity projection of confocal z-stack depict localization of *nhr-67>NHR-67::mCherry* in the two inner somatic gonadal AC/VU cells and the two outer VU cells (Kimble and Hirsh, 1979) (bottom). Illustration of *nhr-67>NHR-67::mCherry* positive cells (red nuclei) in the L2 somatic gonad (bottom) Scale bar, 5 μ m.

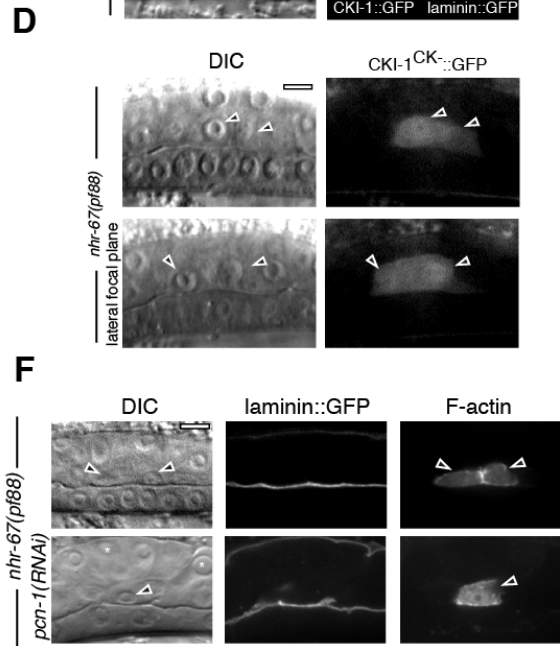
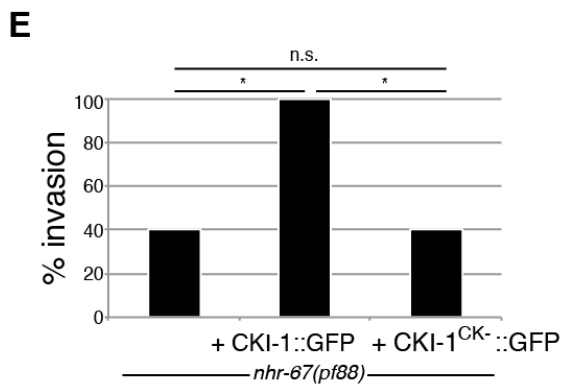
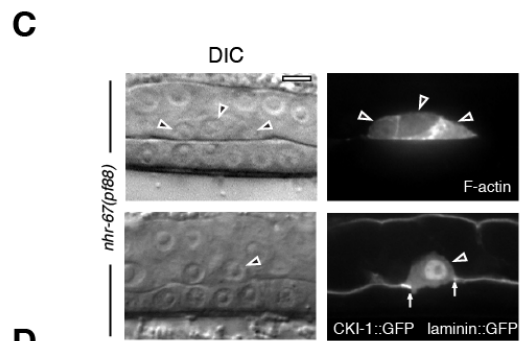
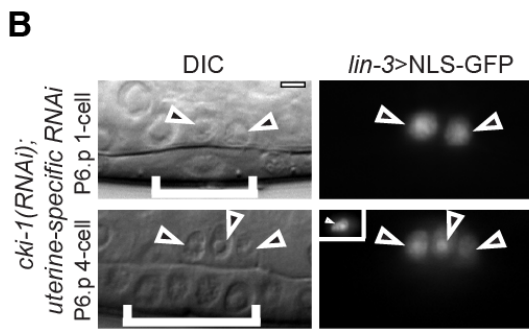
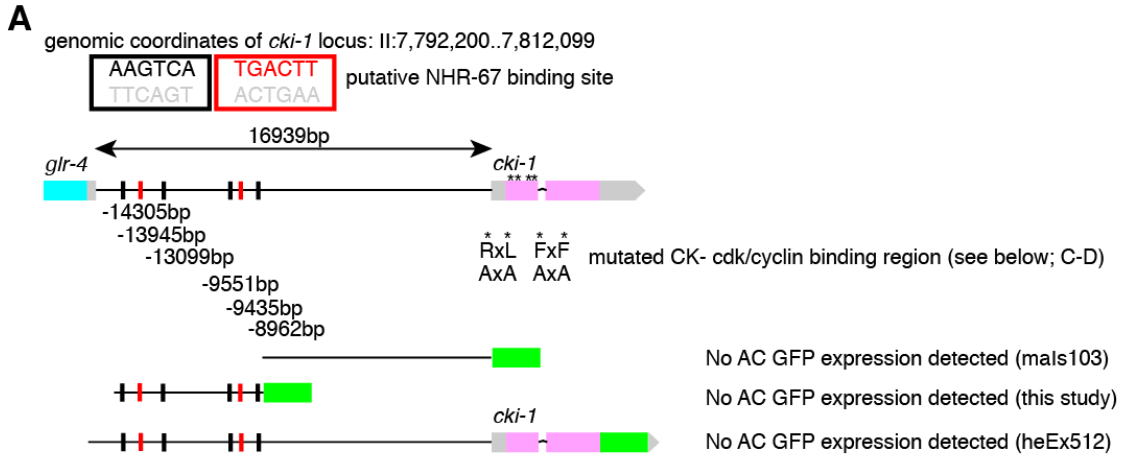


Figure S2. *cki-1* is required in the AC to maintain G1 arrest. Related to Figure 2.

(A) Genomic organization of *cki-1* locus. Schematic of the *cki-1* locus in the *C. elegans* genome depicts the location of six putative NHR-67 binding sites (Sarin et al., 2009). Three GFP reporters were examined for GFP expression in the AC. *Consensus amino acids mutated in the CK- cdk/cyclin binding region in the first exon of *cki-1* (Vlach et al., 1997). (B) Depletion of *cki-1* by RNAi results in rare occurrences of multiple non-invading ACs. DIC micrographs (left) and corresponding epifluorescence images (right) depicting expression of *lin-3*>NLS-GFP. *cki-1*(RNAi) results in rare cases (n = 3) of animals with multiple *lin-3*>NLS-GFP-expressing ACs (arrowheads, top), that fail to breach the BM to contact the 1° VPCs (white bracket). Micrographs (bottom) depict the same animal as shown above, imaged 4 hours later at the normal time of AC invasion (inset, alternate focal plane). (C-E) CKI inhibition of cyclin/CDK rescues *nhr-67*(*pf88*) invasion defects. DIC micrographs (left) and corresponding confocal section (right) with reporter as indicated. (C) *nhr-67*(*pf88*) animal alone (top) with multiple non-invading ACs (arrowheads, AC expressing *cdh-3*>mCherry:: moesinABD) and *nhr-67*(*pf88*) expressing *cdh-3*>CKI-1::GFP (bottom) with restored BM breach (visualized by laminin::GFP, arrows). (D) *nhr-67*(*pf88*) animal expressing a form of CKI lacking conserved residues for binding and inhibiting cyclin/CDK complexes (*cdh-3*>CKI-1^{CK-}::GFP (right)) does not restore invasion or maintain cell-cycle arrest--multiple non-invading ACs shown in two focal planes (top and bottom). (E) Percentage of ACs invading in *nhr-67*(*pf88*), *nhr-67*(*pf88*) with CKI-1::GFP and *nhr-67*(*pf88*) with CKI-1^{CK-}::GFP (n > 20 animals examined for each, *P < 0.0001, n.s., not significant P = 1 as compared to *nhr-67*(*pf88*) alone, Fisher's exact test). (F) DIC micrographs (left) and

corresponding confocal section of BM (laminin::GFP, middle) and AC-specific F-actin probe (*cdh-3*>mCherry::moesinABD, right) at the normal time of invasion. An *nhr-67(pf88)* animal (top) has two ACs (arrowheads) that fail to invade. Induction of S-phase arrest by depletion of *pcn-1* blocked cell division in the AC and other uterine cells (*) but did not rescue invasion (intact laminin::GFP, middle). Scale bar, 5 μ m.

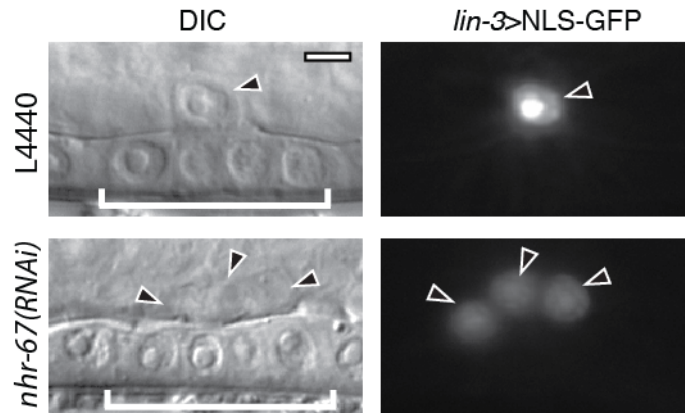


Figure S3. *nhr-67* depleted ACs express *lin-3*. Related to Figure 4. DIC micrographs (left) and corresponding confocal section depicting *lin-3*>NLS-GFP expression (right). ACs (arrowheads) maintain expression of the early marker of AC specification, the EGF ligand, *lin-3*>NLS-GFP, following depletion of *nhr-67* by RNAi. Scale bar, 5 μ m.

Table S1 (see excel file: Matus_TableS1): List of 854 transcription factors targeted by dsRNA from the combined Vidal/Ahringer RNAi libraries. Related to Figure 1.

Table S2 (see excel file: Matus_TableS2): List of 72 transcription factor dsRNA clones that resulted in the presence of Pvl animals following RNAi feeding. Related to Figure 1.

Table S3: AC invasion and proliferation scoring data. Related to Figures 1-6.

Genotype / Treatment	P6.p four-cell stage (mid-to-late L3) ^a	% of animals ^b		n ^c
		1 AC	2+ ACs	
Wild-type (N2)	% Invasion	100	0	> 100
	No Invasion	0	0	
<i>fos-1>RDE-1; rrf-3(pk1426); rde-1(ne219); empty vector (RNAi)</i>	% Invasion	100	0	100
	No Invasion	0	0	
<i>fos-1>RDE-1; rrf-3(pk1426); rde-1(ne219); nhr-67(RNAi)</i>	% Invasion	20	0	97
	No Invasion	0	80	
<i>fos-1>RDE-1; rrf-3(pk1426); rde-1(ne219); hda-1(RNAi)</i>	% Invasion	66	0	94
	No Invasion	34	0	
<i>cdh-3>mCherry::moesinABD; laminin::GFP; empty vector (RNAi)</i>	% Invasion	100	0	100
	No Invasion	0	0	
<i>cdh-3>mCherry::moesinABD; laminin::GFP; nhr-67(RNAi)</i>	% Invasion	24	0	100
	No Invasion	0	76	
<i>nhr-67(pf88); cdh-3>mCherry::moesinABD; laminin::GFP</i>	% Invasion	31	0	100
	No Invasion	0	69*	
<i>nhr-67(pf88); cdh-3>mCherry::moesinABD; laminin::GFP; nhr-67(RNAi)</i>	% Invasion	24	0	103
	No Invasion	0	76*	
<i>nhr-67(pf88); cdh-3>H2B::dendra</i>	% Invasion	31	2	51
	No Invasion	0	67	
<i>nhr-67(pf88); QUAS>nhr-67::venus; cdh-3>QS::SL2::mCherry, QF::SL2::mCherry (- quinic acid)</i>	% Invasion	48	3	31
	No Invasion	0	49	
<i>nhr-67(pf88); QUAS>nhr-67::venus; cdh-3>QS::SL2::mCherry, QF::SL2::mCherry (+ quinic acid)</i>	% Invasion	100	0	25
	No Invasion	0	0	
<i>nhr-67(pf88); cdh-3>CKI-1::GFP</i>	% Invasion	100	0	50
	No Invasion	0	0	
<i>nhr-67(pf88); cdh-3>CKI-1^{CK-}::GFP; myo-2>mCherry</i>	% Invasion	40	0	20
	No Invasion	0	60	
<i>hda-1(RNAi); cdh-3>CKI-1::GFP</i>	% Invasion	74	0	127
	No Invasion	26	0	
<i>nhr-67(pf88); hydroxyurea (25mM)</i>	% Invasion	54	2	87
	No Invasion	31	13	
<i>nhr-67(pf88); pcn-1(RNAi)</i>	% Invasion	37	4	132
	No Invasion	9	50	

<i>nhr-67(pf88); cdk-1(RNAi)</i>	% Invasion	42	0	50
	No Invasion	48	10	
<i>nhr-67(pf88); hsp>CKI-1::GFP (no heat shock control)</i>	% Invasion	30	0	10
	No Invasion	0	70	
<i>nhr-67(pf88); hsp>CKI-1::GFP (heatshock)</i>	% Invasion	35	65	14
	No Invasion	0	0	

^a AC invasion was scored by assessing the presence of a basement membrane (BM) breach using either DIC optics or laminin::GFP.

^b The number of ACs was determined using either DIC optics or the early AC-specification reporters *lin-3>NLS::GFP*, *cdh-3^{l.5}>mCherry::PLCδ^{PH}* or *cdh-3>mCherry::moesinABD*.

^c Number of animals examined for each genotype.

* not significant $P = 0.18$ as compared to *nhr-67(pf88); cdh-3>mCherry::moesinABD; laminin::GFP* alone, Fisher's exact test

Table S4. Extrachromosomal arrays and integrated strains generated. Related to Experimental Procedures.

Ex ^a designation	Is ^b designation	PCR fusion created	Injected conc. (ng/μl)	Co-injection marker(s)
qyEx271	qyIs270	<i>cdh-3 > H2B::dendra^c</i>	25	unc-119+
qyEx241	qyIs347	<i>cdh-3 > QS::SL2::mCherry^c</i>	12	unc-119+
qyEx241	qyIs347	<i>cdh-3 > QF::SL2::mCherry^c</i>	12	unc-119+
qyEx277	qyIs349	<i>QUAS > NHR-67::venus^c</i>	10	unc-119+, <i>myo-2 > mCherry</i>
qyEx211	qyIs193	<i>cyd-1 > GFP^c</i>	10	unc-119+
qyEx212	qyIs196	<i>cdk-4 > GFP^c</i>	10	unc-119+
qyEx238	qyIs225	<i>cdh-3 > mCherry::moesinABD^c</i>	50	unc-119+
qyEx239	qyIs227	<i>cdh-3 > mCherry::moesinABD^c</i>	5	unc-119+
qyEx273	qyIs275	<i>hsp-16-41 > CKI-1::GFP^d</i>	25	unc-119+, <i>myo-2 > mCherry</i>
bmdEx1	n/a	<i>cdh-3 > CKI-1^{CK-}::GFP^d</i>	1	HygR+, <i>myo-2 > mCherry</i>
qyEx316	qyIs301	<i>pat-3 > GFP^c</i>	0.1	unc-119+
qyEx201	qyIs200	<i>zmp-3 > ZMP-3 :: GFP^c</i>	25	unc-119+
qyEx199	qyIs192	<i>zmp-6 > GFP^c</i>	25	unc-119+

^a Ex signifies an extrachromosomal transgenic line

^b Is denotes a stability integrated transgenic line

^c 3' UTR from the *unc-54* gene was included at the 3' end of the construct

^d The endogenous 3' UTR was used

Table S5. Primer sequences and templates used for all PCR fusions generated. Related to Experimental Procedures.

Primer sequence	Primer type	Amplicon	Template
5'-GGTTTGTAGAATGTGTTGTTCC-3'	<i>forward</i>		
5'-CTCATATCGAAGGTCTGGTGCC-3'	<i>forward nested</i>	<i>cdh-3</i> promoter (5 kb)	JP38
5'-CGTATTGTCATCTATTACAGATTGATCTGG-3'	<i>reverse</i>		
5'-GAATAGATGACAATACGATGTCTTCTGCTCGTC-3'	<i>cdh-3</i> extension, <i>forward</i>		
5'-TCATAGAGATATGCACCCATAC-3'	<i>reverse</i>	H2B::GFP	pLZ6
5'-TCAATATGCGGTGTACTTCTGG-3'	<i>reverse nested</i>		
5'-GAATAGATGACAATACGATGCCACCAAAGCCATCTG	<i>cdh-3</i> extension, <i>forward</i>		
5'-CAGGAAACAGCTATGACCATG-3'	<i>reverse</i>	H2B::dendra	pDQM1
5'-GCGCAATTAACCCTCACTAAAGGGA-3'	<i>reverse nested</i>		
5'-GAATAGATGACAATACGATGTCTTCTGCTCGT-3'	<i>cdh-3</i> extension, <i>forward</i>		
5'-GTCCGTTCCAAGGTCTTCTCG-3'	<i>reverse</i>	CKI-1 ^{CK-} ::GFP	pDQM2
5'-TCACGCAATCTTCACGCAATGTC-3'	<i>reverse nested</i>		
5'-GAATAGATGACAATACGATGCCACCAAAGCCATCTG- 3'	<i>hsp-16-41</i> extension, <i>forward</i>		
5'-GTCCGTTCCAAGGTCTTCTCG-3'	<i>reverse</i>	CKI-1::GFP	fosmid WRM0626bF02
5'-TCACGCAATCTTCACGCAATGTC-3'	<i>reverse nested</i>		
5'-TTGACACCGTTCTCTGAGCTGG-3'	<i>forward</i>		
5'-TAACCACAAAAC-3'	<i>forward nested</i>	<i>cdt-1</i> > CDT-1::GFP	N2 genomic DNA
5'-AATTCTTCTCCTTTACTCATATAAATTTAAATC-3'	<i>gfp</i> extension, <i>reverse</i>		
5'-ATATAAAAAAACTTTTCAC-3'	<i>forward</i>		
5'-CTCCCTTCTATACTA-3'	<i>reverse</i>	GFP	pPD95_81
5'-CTACTATCCCTACCCCTT 3'	<i>reverse nested</i>		
5'-CTTCCTTATCTCCTC-3'	<i>forward</i>		
5'-AAATCAACCCATAA-3'	<i>forward nested</i>	<i>pat-3</i> promoter	N2 genomic DNA
5'-AATTCTTCTCCTTTACTCATTATCCTA-3'	<i>reverse</i>		
5'-AGACGATGAGCCAACCTGGTG-3'	<i>forward</i>		
5'-TGCATGAAGCAGTTGCAGAA-3'	<i>forward nested</i>	<i>zmp-3</i> > ZMP-3::GFP	N2 genomic DNA
5'-AAGTTCTTCTCCTTTACTCATAACGGCGATATAACTGG-3'	<i>reverse</i>		
5'-TTTGAAAGGGCGGAGAAGTC-3'	<i>forward</i>		
5'-CCTCAAGGCAATGCTTCTCC-3'	<i>forward nested</i>	<i>zmp-6</i> promoter	N2 genomic DNA
5'-AAGTTCTTCTCCTTTACTCATTCTCCCTGCTCCCGAAACC-3'	<i>reverse</i>		

Movie S1. *nhr-67*-depleted ACs divide. Related to Figure 1. Lateral view time-lapse shows ACs with markers for F-actin (*cdh-3*>mCherry::moesinABD, green) and Histone H2B (*cdh-3*>H2B::GFP, magenta) in wild-type (left) and *nhr-67*(*RNAi*)-treated animals (right) prior to invasion. The two ACs in the *nhr-67*-depleted animal undergo one round of division. Images were acquired using a spinning disc confocal microscope (CSU-10 scan head; Yokogawa, mounted on a Zeiss AxioImager compound microscope). A 60 minute time lapse is shown. Time points were acquired every 30s. Movies were constructed from projections of confocal z-section (step size of 0.5 μ m). The dashed line indicates the position of the BM. Scale bar, 5 μ m.

Supplemental References

- Greiss, S., and Chin, J.W. (2011). Expanding the genetic code of an animal. *Journal of the American Chemical Society* *133*, 14196-14199.
- Kimble, J., and Hirsh, D. (1979). The Postembryonic Cell Lineages of the Hermaphrodite and Male Gonads in *Caenorhabditis elegans*. *Developmental biology* *70*, 396-417.
- Kirouac, M., and Sternberg, P.W. (2003). cis-Regulatory control of three cell fate-specific genes in vulval organogenesis of *Caenorhabditis elegans* and *C. briggsae*☆. *Developmental biology* *257*, 85-103.
- Matus, D.Q., Li, X.Y., Durbin, S., Agarwal, D., Chi, Q., Weiss, S.J., and Sherwood, D.R. (2010). In vivo identification of regulators of cell invasion across basement membranes. *Sci Signal* *3*, ra35.
- Rual, J.F. (2004). Toward Improving *Caenorhabditis elegans* Phenome Mapping With an ORFeome-Based RNAi Library. *Genome Research* *14*, 2162-2168.
- Sarin, S., Antonio, C., Tursun, B., and Hobert, O. (2009). The *C. elegans* Tailless/TLX transcription factor *nhr-67* controls neuronal identity and left/right asymmetric fate diversification. *Development (Cambridge, England)* *136*, 2933-2944.
- Sherwood, D.R., Butler, J., Kramer, J., and Sternberg, P. (2005). FOS-1 Promotes Basement-Membrane Removal during Anchor-Cell Invasion in. *Cell* *121*, 951-962.
- Sherwood, D.R., and Sternberg, P.W. (2003). Anchor cell invasion into the vulval epithelium in *C. elegans*. *Developmental cell* *5*, 21-31.
- Vlach, J., Hennecke, S., and Amati, B. (1997). Phosphorylation-dependent degradation of the cyclin-dependent kinase inhibitor p27. *The EMBO journal* *16*, 5334-5344.
- Wei, X., Potter, C.J., Luo, L., and Shen, K. (2012). Controlling gene expression with the Q repressible binary expression system in *Caenorhabditis elegans*. *Nat Methods* *9*, 391-395.